74N29329

NASA TECHNICAL NOTE

NASA TN D-7622

NASA TN D-7622

# CURVE FITS OF PREDICTED INVISCID STAGNATION-POINT RADIATIVE HEATING RATES, COOLING FACTORS, AND SHOCK STANDOFF DISTANCES FOR HYPERBOLIC EARTH ENTRY

*by John T. Suttles, Edward M. Sullivan, and Stephen B. Margolis*

*Langley Research Center*
*Hampton, Va. 23665*



NATIONAL AERONAUTICS AND SPACE ADMINISTRATION • WASHINGTON, D. C. • JULY 1974

| 1. Report No. NASA TN D-7622 | 2. Government Accession No. | 3. Recipient's Catalog No. |
|---|---|---|
| 4. Title and Subtitle CURVE FITS OF PREDICTED INVISCID STAGNATION-POINT RADIATIVE HEATING RATES, COOLING FACTORS, AND SHOCK STANDOFF DISTANCES FOR HYPERBOLIC EARTH ENTRY | | 5. Report Date July 1974 |
| | | 6. Performing Organization Code |
| 7. Author(s) John T. Suttles, Edward M. Sullivan, and Stephen B. Margolis | | 8. Performing Organization Report No. L-9315 |
| | | 10. Work Unit No. 502-27-01-01 |
| 9. Performing Organization Name and Address NASA Langley Research Center Hampton, Va. 23665 | | 11. Contract or Grant No. |
| | | 13. Type of Report and Period Covered Technical Note |
| 12. Sponsoring Agency Name and Address National Aeronautics and Space Administration Washington, D.C. 20546 | | 14. Sponsoring Agency Code |
| 15. Supplementary Notes | | |

16. Abstract

Curve-fit formulas are presented for the stagnation-point radiative heating rate, cooling factor, and shock standoff distance for inviscid flow over blunt bodies at conditions corresponding to high-speed earth entry. The data which were curve fitted were calculated by using a technique which utilizes a one-strip integral method and a detailed nongray radiation model to generate a radiatively coupled flow-field solution for air in chemical and local thermodynamic equilibrium. The range of free-stream parameters considered were altitudes from about 55 to 70 km and velocities from about 11 to 16 km/sec. Spherical bodies with nose radii from 30 to 450 cm and elliptical bodies with major-to-minor axis ratios of 2, 4, and 6 were treated.

Power-law formulas are proposed and a least-squares logarithmic fit is used to evaluate the constants. It is shown that the data can be described in this manner with an average deviation of about 3 percent (or less) and a maximum deviation of about 10 percent (or less). The curve-fit formulas provide an effective and economic means for making preliminary design studies for situations involving high-speed earth entry.

| 17. Key Words (Suggested by Author(s)) | 18. Distribution Statement |
|---|---|
| Aerodynamic heat transfer<br>Radiative heat flux<br>Stagnation flow<br>Equilibrium flow<br>Curve-fit formulas | Unclassified – Unlimited<br><br>STAR Category 33 |

| 19. Security Classif. (of this report) | 20. Security Classif. (of this page) | 21. No. of Pages | 22. Price* |
|---|---|---|---|
| Unclassified | Unclassified | 41 | $3.25 |

*For sale by the National Technical Information Service, Springfield, Virginia 22151

# CURVE FITS OF PREDICTED INVISCID STAGNATION-POINT RADIATIVE HEATING RATES, COOLING FACTORS, AND SHOCK STANDOFF DISTANCES FOR HYPERBOLIC EARTH ENTRY

By John T. Suttles, Edward M. Sullivan,
and Stephen B. Margolis
Langley Research Center

## SUMMARY

Curve-fit formulas are presented for the stagnation-point radiative heating rate, cooling factor, and shock standoff distance for inviscid flow over blunt bodies at conditions corresponding to high-speed earth entry. The data which were curve fitted were calculated by using a technique which utilizes a one-strip integral method and a detailed nongray radiation model to generate a radiatively coupled flow-field solution for air in chemical and local thermodynamic equilibrium. The range of free-stream parameters considered were altitudes from about 55 to 70 km and velocities from about 11 to 16 km/sec. Spherical bodies with nose radii from 30 to 450 cm and elliptical bodies with major-to-minor axis ratios of 2, 4, and 6 were treated.

Power-law formulas are proposed and a least-squares logarithmic fit is used to evaluate the constants. It is shown that the data can be described in this manner with an average deviation of about 3 percent (or less) and a maximum deviation of about 10 percent (or less). The curve-fit formulas provide an effective and economic means for making preliminary design studies for situations involving high-speed earth entry.

## INTRODUCTION

One of the problems encountered by hypervelocity heat-shield designers and trajectory analysts is that of calculating the radiative flux to an entry body. For economic reasons, it is desirable to conduct studies and preliminary design work by using simplified approaches and correlation equations such as those in reference 1. The radiative heating-rate correlation used in reference 1 was derived from early heating-rate predictions which were based on a transparent, constant property shock layer. More recent studies have shown the early work to be grossly in error for high-speed entry problems. The survey given in reference 2 shows that for high-speed entries a heating-rate analysis must include the combined effects of shock-layer radiative cooling (which results in properties varying across the shock layer), nongray self-absorption, continuum radiation, and atomic line radiation to be valid.

Numerous analyses are now available (e.g., refs. 3 to 8) which include these important effects for inviscid, stagnation region flow. Several of these techniques (refs. 4 to 6) have used approximate absorption-coefficient models for the radiation calculations in the interest of making engineering simplifications to this complex problem. However, these approaches are not in a convenient form for designers and analysts who desire estimates of shock-layer radiative heat transfer without resorting to lengthy computer solutions. Based on the success of the graphical correlation in reference 9, it is reasonable to expect that a simple analytic expression for radiative heating rates, such as that used in reference 1, can be derived by curve fitting the results of detailed computer solutions. Therefore, such an effort was undertaken.

In addition to heating rates an effort was made to curve fit the cooling factor since it is believed that the results presented in this form will be of more lasting value than the heating-rate results. The cooling factor is simply the ratio of the heating rate for a nonadiabatic shock layer to the heating rate for an adiabatic shock layer with the heating rates based on the same radiation model, body size, and flight conditions. (It is well known that for hypervelocity flows nonadiabatic effects significantly reduce the radiative heating compared to the heating calculated by assuming adiabatic conditions.)

Olstad (refs. 4 and 9) has demonstrated that the cooling factor can be correlated as a function of the heating rate for an adiabatic shock layer normalized by the free-stream kinetic-energy flux $\left(\frac{1}{2} \rho_\infty V_\infty{}^3\right)$. The twofold usefulness of the cooling factor was also suggested by Olstad (ref. 9). First, the use of the cooling factor minimizes the effects of the radiation model used in the calculation; heating rates which have significantly different values as a consequence of the use of different radiation models show good agreement when compared on the cooling-factor basis. This rationale is used for the comparison of results in the present report. Second, because the cooling factor has this property of bringing radiative heating rates calculated with diverse radiation models to a common base, it can be used in conjunction with an adiabatic heating rate calculated with the best available radiation model to calculate the nonadiabatic heating rate. With this approach it is not necessary to use time-consuming coupled flow-field solutions to obtain radiative heating rates, nor is it necessary to recalculate the cooling factors as improvements are made in radiation models.

Since inviscid shock-standoff-distance values are obtained when heating rates and cooling factors are calculated, a curve fit for this quantity was derived also. The shock standoff distance is of interest to heat-shield designers, for example, in evaluating the effects of a probe extending from the body into the shock layer. Also, flow-field analysts find that the shock standoff distance has numerous uses, two of which are for comparing various results and for initiating iterative solutions.

The present report presents the results of curve fitting information on calculated heating rate, cooling factor, and shock standoff distance with simple expressions involving free-stream conditions and vehicle geometry parameters. The calculations were made by using a radiatively coupled flow-field computer program (ref. 3) which includes a detailed nongray radiation model (refs. 10 and 11). The range of free-stream parameters considered were altitudes from about 55 to 70 km and velocities from about 11 to 16 km/sec. Spherical bodies with nose radii from 30 to 450 cm and elliptical bodies with major-to-minor axis ratios of 2, 4, and 6 were treated. The simple form used for the curve fits is suitable for hand calculation with a slide rule or electronic desk calculator and can be readily included in a parametric analysis.

## SYMBOLS

| | |
|---|---|
| $a_{ji}$ | coefficient matrix of equation (5) |
| $A_i$ | constants used in heating-rate curve fit (see eq. (1)) |
| $b_{ji}$ | coefficient matrix of equation (8) |
| $B_i$ | constants used in cooling-factor curve fit (see eq. (7)) |
| $c_{ji}$ | coefficient matrix of equation (10) |
| $C_i$ | constants used in shock-standoff-distance curve fit (see eq. (9)) |
| $D_j$ | constant vector of equation (5) |
| e | base for natural logarithms (e = 2.71828 . . .) |
| E | total-error measure (see eq. (4)) |
| $F_C$ | cooling factor, ratio of nonadiabatic-to-adiabatic heating rates |
| $G_j$ | constant vector of equation (8) |
| $H_j$ | constant vector of equation (10) |

| | |
|---|---|
| $i$ | index used for constants in curve-fit equations |
| $j$ | index used for equations resulting from minimization procedure |
| $K$ | constant in functional form assumed for curve-fit equations |
| $n$ | index used to identify individual data points which are to be curve fitted (case number) |
| $N$ | total number of data points for a curve fit |
| $q_R$ | radiative heating rate, $W/cm^2$ |
| $r$ | axis ratio of elliptical bodies, free-stream velocity always oriented normal to major axis |
| $R_B$ | body nose radius, cm |
| $V_\infty$ | free-stream velocity, km/sec |
| $X$ | denotes any of quantities to be curve fitted |
| $\delta$ | stagnation-point shock standoff distance, cm |
| $\epsilon_n$ | error of curve fit at the nth data point |
| $\rho_\infty$ | free-stream density (obtained from 1962 standard atmosphere for a given altitude), $g/cm^3$ |

Subscripts:

| | |
|---|---|
| C | curve fit |
| D | data |
| r | axis ratio |
| $\delta$ | shock standoff distance |

Superscripts:

a,b,c exponents in the functional form assumed for curve-fit equations

## METHOD

The data to be curve fitted were obtained from solutions of the inviscid radiating flow field in the stagnation region of a blunt body (fig. 1), which is entering the Earth's atmosphere. These solutions were obtained by using the one-strip integral method of reference 3 which incorporates the nongray radiation model of reference 10 as a subroutine. The radiation model ("RATRAP") is described in further detail and compared with other models in reference 11. The computational method is for the inviscid flow of air in chemical and local thermodynamic equilibrium. The radiation calculations assume a plane slab shock-layer geometry and neglect absorption by the air upstream of the shock layer and byproducts of ablation at the body surface. Discussion of the importance of these effects can be found in reference 2.

The data on which the curve fits are based are given in table I. The free-stream conditions, velocity and density (density determined from 1962 standard atmosphere for a given altitude), were picked to cover the range of interest for high-speed entry cases where radiative heating will be important. Figure 2 illustrates the conditions chosen: a typical manned planetary-return lifting-entry trajectory (ref. 12), a range of high-velocity ballistic-entry trajectories (from an unpublished study), and a matrix of cases which span the trajectories. The body sizes were selected from results of an unpublished study and cover a range of interest from small unmanned probes of preliminary flight-test vehicles to large manned spacecraft. Thus, the curve fits should be of value for a wide range of applications.

The effort was undertaken on the premise that if sufficient data were available it would be possible to write a curve-fit equation of the form

$$X = K\rho_\infty{}^a R_B{}^b V_\infty{}^c$$

where $X$ represents either the heating rate, cooling factor, or the standoff distance and $a$, $b$, and $c$ may be allowed to vary with the free-stream conditions and/or body size. This form has been used to correlate convective heating rates (see, e.g., ref. 13), and it is well suited for calculations made with either a slide rule or electronic desk calculator. It can also be readily programed for repetitive calculations on a digital computer.

## CURVE-FIT EQUATIONS

### Heating Rates

Spherical bodies.- A curve fit of the stagnation-point radiative heating rate $q_R$ with the free-stream velocity $V_\infty$, free-stream density $\rho_\infty$, and the body radius $R_B$ was obtained by fitting a multidimensional curve through the spherical body data (cases 1 to 91) in table I. Based on a preliminary analysis, the functional form

$$q_{R,C} = e^{A_1} \rho_\infty^{A_2+A_3V_\infty} R_B^{A_4+A_5V_\infty+A_6V_\infty^2} V_\infty^{A_7+A_8V_\infty+A_9V_\infty^2} \tag{1}$$

was assumed and the constants $A_1, A_2, \ldots, A_9$ were found by a least-squares analysis. To facilitate application of the least-squares method, equation (1) was first linearized with respect to the $A_i$ values by taking logarithms as follows:

$$\begin{aligned} \ln q_{R,C} = A_1 &+ A_2 \ln \rho_\infty + A_3V_\infty \ln \rho_\infty + A_4 \ln R_B + A_5V_\infty \ln R_B \\ &+ A_6V_\infty^2 \ln R_B + A_7 \ln V_\infty + A_8V_\infty \ln V_\infty + A_9V_\infty^2 \ln V_\infty \end{aligned} \tag{2}$$

The error function for the least-squares method is, therefore,

$$\epsilon_n = \ln q_{R,D}(n) - \ln q_{R,C}(n) \tag{3}$$

where $q_{R,D}(n)$ is the value of $q_R$ corresponding to the nth data point $[\rho_\infty(n),\ V_\infty(n),$ and $R_B(n)]$ from table I, and $q_{R,C}(n)$ is the $q_R$ value obtained from the curve fit (eq. (1)) for the nth point. The total-error measure in the method is given by

$$E = \sum_{n=1}^{N} \epsilon_n^2 \tag{4}$$

and is to be minimized with respect to each of the $A_i$ values. The minimization leads to a set of linear simultaneous equations for the $A_i$ values whose matrix form is as follows:

$$a_{ji}A_i = D_j \qquad (i,j = 1, 2, \ldots, 9) \tag{5}$$

where the $A_i$ values have previously been defined and the coefficient matrix $a_{ji}$ and $D_j$ values are given in table II. The elements of the coefficient matrix involve summations of functions involving $\rho_\infty(n)$, $R_B(n)$, and $V_\infty(n)$; and the $D_j$ values involve summations of functions involving $\rho_\infty(n)$, $R_B(n)$, $V_\infty(n)$, and $q_{R,D}(n)$. In each case, the summations are over the N data points. Equation (5) was solved by inverting the coefficient matrix $a_{ji}$. The results for the $A_i$ values are given in the appendix, and the results using equation (1) with the $A_i$ values are given in table III(a) for the 91 points used. A comparison of $q_{R,D}$ with $q_{R,C}$ in table III(a) shows an average deviation of approximately 3 percent. Also, of the 91 data points only 3 have deviations larger than 7 percent, and these are for small bodies at high altitudes – conditions for which the calculated radiative heat-transfer rates tend to be very low and the inaccuracy may be large.

Elliptical bodies.- The curve fits presented were based on the data for spherical bodies given in table I. Data are given in table I (cases 102 to 150) for elliptical bodies with axis ratios of 2, 4, and 6. For the elliptical shapes the free-stream velocity is normal to the semimajor axis and $R_B$ is the stagnation-point radius of curvature. When the curve fit for the spherical-body data was applied to the nonspherical-body data, a systematic error appeared which depended on the axis ratio. This error was attributed to the fact that the axis ratio influences the tangential velocity gradient and the shock standoff distance. It was found possible to compensate for this effect by use of a correction factor (called the shape factor) which is a linear function of the axis ratio. The shape factor was obtained by calculating $q_{R,C}$ for each of the nonspherical-body cases by using equation (1) and forming the ratio of $q_{R,C}$ to $q_{R,D}$. These ratios were collected into groups of data corresponding to common axis ratios, and simple averages for each group were determined. The value of $\overline{\frac{q_{R,C}}{q_{R,D}}}$ for the spherical bodies (unit axis ratio) was taken to be 1.0. Thus, values for the shape factor were generated for axis ratios of 1, 2, 4, and 6. A linear function was assumed for the variation of the shape factor with axis ratio, and a least-squares curve-fit method was used to find the slope and intercept. Figure 3 presents the data used in the shape-factor calculations and the line obtained from the least-squares fit. With the resulting shape factor, the expression for $q_{R,C}$ for nonspherical bodies is

$$q_{R,C,r} = \frac{q_{R,C}}{(0.955859 + 0.03645r)} \tag{6}$$

which is used for $1 < r \leqq 6$. It is noted that the shape factor is not precisely 1.0 at unit axis ratio since this condition was used merely as a data point rather than as a constraint for the curve fit.

The $q_{R,C,r}$ values are compared with the corresponding $q_{R,D}$ values in table III(b). The results are excellent with an average deviation of 3 percent and a maximum of 8 percent for the cases where $R_B$, $\rho_\infty$, and $V_\infty$ are in the range for which the $A_i$ values were originally calculated.

## Cooling Factors

A curve fit for the cooling factor $F_C$ was derived from the 53 cases in table I for which $F_C$ values were given. The curve-fit formula for $F_C$ as a function of $\rho_\infty$, $V_\infty$, and $R_B$ was obtained in the same manner as that for $q_R$. A function of the form

$$F_{C,C} = e^{B_1} \rho_\infty^{\,B_2+B_3R_B+B_4R_B^2+B_5R_B^3} R_B^{\,B_6} V_\infty^{\,B_7} \tag{7}$$

was assumed based on a preliminary data analysis. Taking the logarithm of equation (7) and applying the least-squares method resulted in a set of equations for the $B_i$ values whose matrix form is as follows:

$$b_{ji}B_i = G_j \qquad (i,j = 1, 2, \ldots, 7) \tag{8}$$

where the $B_i$ values are the constants appearing in equation (7) and the coefficient matrix $b_{ji}$ and $G_j$ values are given in table IV. The elements of the coefficient matrix involve summations over the N data points of functions involving $\rho_\infty(n)$, $V_\infty(n)$, and $R_B(n)$, whereas the $G_j$ values involve summations of functions involving $\rho_\infty(n)$, $V_\infty(n)$, $R_B(n)$, and $F_{C,D}(n)$. Equation (8) was solved by inverting the coefficient matrix $b_{ji}$. The results for the $B_i$ values are presented in the appendix, and the results using equation (7) with the $B_i$ values to compute $F_{C,C}$ are given in table V. A comparison of $F_{C,C}$ with $F_{C,D}$ is also given. These results for the cooling factor have an average deviation of approximately 3 percent and a maximum deviation of about 10 percent.

## Shock Standoff Distances

Spherical bodies.- A curve-fit formula for the shock standoff distance at the stagnation streamline as a function of $\rho_\infty$, $V_\infty$, and $R_B$ was obtained in the same manner as those for $q_R$ and $F_C$. Ninety-one spherical-body cases (cases 1 to 91) were used. A function of the form

$$\delta_C = e^{C_1} \rho_\infty^{\,C_2+C_3V_\infty} R_B^{\,C_4+C_5V_\infty} V_\infty^{\,C_6+C_7V_\infty+C_8V_\infty^2} \tag{9}$$

was assumed based on a preliminary analysis of the available standoff-distance data. Again, by taking the logarithm of the assumed function and applying the least-squares method, a set of equations for the $C_i$ values was obtained. The matrix form of these equations is as follows:

$$c_{ji}C_i = H_j \qquad (i,j = 1, 2, \ldots, 8) \tag{10}$$

where the $C_i$ values are the constants appearing in equation (9) and the coefficient matrix $c_{ji}$ and $H_j$ values are given in table VI. The elements of the coefficient matrix involve summations over the N data points of functions involving $\rho_\infty(n)$, $R_B(n)$, and $V_\infty(n)$; whereas the $H_j$ values involve summations of functions involving $\rho_\infty(n)$, $R_B(n)$, $V_\infty(n)$, and $\delta_D(n)$. Equation (10) was solved by inverting the matrix $c_{ji}$, and the $C_i$ values are given in the appendix. Table VII(a) gives a comparison of the original standoff-distance data $\delta_D$ with $\delta_C$ values calculated by using equation (9) and the derived $C_i$ values. The results show that when compared to $\delta_D$ the corresponding $\delta_C$ values have an average deviation of about 1 percent with a maximum deviation of about 5 percent.

Elliptical bodies.- A shape factor for the standoff distance for the nonspherical-body cases was derived in the same manner as that for the heating-rate correlation. The resultant expression for the shock standoff distance for the elliptical bodies is

$$\delta_{C,r} = \frac{\delta_C}{(0.825784 + 0.14816r)} \tag{11}$$

which is applied for $1 < r \leqq 6$. The data from which the shape factor for equation (11) was derived are shown in figure 4. The comparison of $\delta_{C,r}$ with $\delta_{D,r}$ given in table VII(b) shows that the curve-fit values have an average deviation of 4 percent compared to the original data.

## DISCUSSION

As shown in tables III, V, and VII the curve-fit equations give good representations of the basic data (table I) in the ranges specified in the appendix. In this section the basic data and/or the curve fits will be compared with other available data. In addition, the cooling-factor curve fit was studied extensively in order to establish its sensitivity to out-of-range conditions. The results of this study are also presented.

### Heating Rates

Radiative heat-transfer calculations are known to be significantly influenced by both the flow-field calculation technique and the radiation transfer model. The basic data (table I) for heating rate and standoff distance were calculated by using the one-strip integral technique of reference 3, which includes the radiation model of reference 10. Results from calculations using these techniques have been compared with several other methods and these comparisons have been published (e.g., refs. 3, 7, and 8). The general finding is that the one-strip integral technique produces results which compare very well with other techniques, provided that the same radiation model is used. Thus, it can be concluded that the fluid mechanics of the method are adequate.

The effects resulting from the use of different radiation models have also been explored (refs. 3 and 11). It has been found that the calculated heating rates for a given set of conditions can differ by 50 percent or more. This result is not surprising when one considers the diversity in the amount of detail programed into various radiation models. In view of the lack of experimental data, at the conditions of interest here, it is difficult to assess which of the available radiation models gives the most accurate results and which provides the best compromise between accuracy and required computer time. For these reasons the present heating-rate results are not compared with previously published values. Instead, such comparisons will be made on a cooling-factor basis in the next section.

## Cooling Factors

As indicated in the "Introduction," Olstad (ref. 9) has shown that when the cooling factor $F_C$ is taken as a basis, good agreement is obtained between results calculated by using different radiation models. Therefore, the $F_C$ curve fit of the present report will be compared to the charts of $F_C$ presented by Olstad in reference 9. It is emphasized that to derive heating rates from $F_C$ values a companion calculation of the adiabatic radiative heating rate is required. That is,

$$\left(q_R\right)_{nonadiabatic} = F_C\left(q_R\right)_{adiabatic} \tag{12}$$

and $\left(q_R\right)_{adiabatic}$ does not require a time-consuming coupled flow-field solution. Since $F_C$ is relatively insensitive to the radiation model (ref. 9), this allows the user to select the model most appropriate to his purpose to determine the adiabatic value. If the user desires to accept the radiation model applied in the calculation of the basic data of this report, he can simply use the heating-rate curve fit presented herein.

The basic data have been curve fitted wherever possible (the 53 cases having $F_C$ values in table I) in terms of $F_C$; the resulting curve-fit equation is given in the appendix. It can be seen (table V) that the agreement between the basic data and the curve fit is excellent with a maximum error of approximately 10 percent. As an independent check, a large number (180) of cooling-factor values were calculated by using the curve-fit equation (eq. (7)) and compared with the curves given in reference 9. Figures 5, 6, and 7 show the results of these calculations. Note that some calculations shown in the figures are out of the range of the correlation. This was done to show the sensitivity of the curve fit. (The calculations also included cases with $R_B = 800$ cm; however, they produced an unreasonably small $F_C$ and have not been plotted.) In figure 5 it is seen that the values from the curve fit for those cases where all three parameters are within the ranges specified in the appendix are in excellent agreement with the results of reference 9. The maximum difference is approximately 17 percent for one case of a 30-cm body at an altitude near the upper limit of the altitude range. The values from figures 5, 6, and 7 for cases where one or more of the parameters are out of range show that the curve fit is most sensitive to body size and least sensitive to velocity.

In view of the results shown in figures 5, 6, and 7, the authors believe that the cooling-factor curve fit is accurate provided the ranges specified in the appendix are not exceeded.

### Shock Standoff Distances

Figure 8 presents a comparison of the shock standoff distances from the basic data (table I), the curve-fit equation (the appendix), and the results of Callis (ref. 6) for $\rho_\infty = 1.225 \times 10^{-7}$ g/cm$^3$ and for $V_\infty = 15.24$ km/sec and 12.19 km/sec. The basic data do not contain identically corresponding results, and, therefore, data for the closest conditions $\left(\rho_\infty = 1.2959 \times 10^{-7}\right.$ g/cm$^3$ and $V_\infty = 15$ km/sec and 12 km/sec$\left.\right)$ are given. It is seen from figure 8 that these slight variations in $V_\infty$ and $\rho_\infty$ have little effect on the comparison. The comparison shows that the curve-fit equation gives an excellent representation of the basic data and, although the trends are different, the basic data and the results of Callis agree within 10 percent or less. A more detailed comparison between the two methods (i.e., Suttles (ref. 3) and Callis (ref. 6)) is given in reference 3, where it is shown that the differences between radiation models can account for a significant difference in the results. Therefore, the variation in the trends of the results in figure 8 are most probably due to the different radiation models used.

Some comparisons were made (but not shown here) between the results of the present work and the results of Callis for bodies smaller $(R_B = 1$ to 30 cm$)$ and for bodies larger $(R_B = 450$ to 1000 cm$)$ than those considered in the curve fits. This comparison indicated that for bodies in the range of $R_B$ from 10 to 30 cm, the results remained in good agreement (10 percent or less); but for smaller bodies and bodies larger than 450 cm, the results began to deviate significantly. It is concluded that, as in the case of the cooling-factor curve fit, the user should be very hesitant in applying the shock-standoff-distance curve fit outside the range of the basic data.

## CONCLUDING REMARKS

Curve-fit formulas are presented for the stagnation-point radiative heating rate, cooling factor, and shock standoff distance for inviscid flow over blunt bodies at conditions corresponding to high-speed earth entry. The data on which the curve fits are based were calculated by using a technique which utilizes a one-strip integral method and a detailed nongray radiation model to generate a radiatively coupled flow-field solution for air in chemical and local thermodynamic equilibrium. The range of free-stream parameters considered were altitudes from about 55 to 70 km and velocities from about 11 to 16 km/sec. Spherical bodies with nose radii of from 30 to 450 cm and elliptical bodies with major-to-minor axis ratios of 2, 4, and 6 were treated.

Power-law formulas are proposed and a least-squares logarithmic fit is used to evaluate the constants. It is shown that the data can be described in this manner with an average deviation of about 3 percent (or less) and a maximum deviation of about 10 percent. A study of the sensitivity of the formulas indicates that they should be used only within the range of the free stream and vehicle geometry parameters of the data. These curve-fit formulas provide an effective and economic means for making preliminary design studies for situations involving high-speed earth entry.

Langley Research Center,
National Aeronautics and Space Administration,
Hampton, Va., April 30, 1974.

## APPENDIX

## CURVE-FIT FORMULAS AND RELATED PARAMETERS

For the convenience of the reader, the curve-fit formulas, the constants derived for the formulas, the ranges of applicability of the formulas, and the average deviation of the formulas from the basic data are listed in this appendix.

### Heating Rates

Formula.- The formula for $q_{R,C}$ in $W/cm^2$ is

$$q_{R,C} = K_r e^{A_1} \rho_\infty^{A_2+A_3V_\infty} R_B^{A_4+A_5V_\infty+A_6V_\infty^2} V_\infty^{A_7+A_8V_\infty+A_9V_\infty^2}$$

Derived constants.-

$$K_r = \begin{cases} \dfrac{1}{(0.955859 + 0.03645r)} & (r \neq 1) \\ 1 & (r = 1) \end{cases}$$

$A_1 = -69.099$ $\qquad$ $A_6 = 0.005381$

$A_2 = 1.320$ $\qquad$ $A_7 = 51.89$

$A_3 = -0.01223$ $\qquad$ $A_8 = -1.558$

$A_4 = 1.688$ $\qquad$ $A_9 = 0.02659$

$A_5 = -0.1796$

Ranges of applicability.-

$\rho_\infty = 1.078 \times 10^{-7}$ to $6.53 \times 10^{-7}$ g/cm$^3$

Altitude = 53.75 to 68.4 km

$R_B$ = 30 to 450 cm

$V_\infty$ = 11 to 16 km/sec

r = 1 to 6

Average deviation.- 3 percent

### Cooling Factors

Formula.- The cooling factor $F_{C,C}$ is dimensionless and is given by

$$F_{C,C} = e^{B_1} \rho_\infty^{B_2+B_3R_B+B_4R_B^2+B_5R_B^3} R_B^{B_6} V_\infty^{B_7}$$

Derived constants.-

$B_1 = -3.679$ $\quad$ $B_5 = 0.000000005567$

$B_2 = -0.3598$ $\quad$ $B_6 = 1.059$

$B_3 = 0.002024$ $\quad$ $B_7 = -1.931$

$B_4 = -0.000005583$

Ranges of applicability.-

$\rho_\infty = 5.61 \times 10^{-7}$ to $8.75 \times 10^{-8}$ g/cm$^3$

Altitude = 55 to 70 km

$R_B$ = 30 to 450 cm

$V_\infty$ = 11 to 16 km/sec

Average deviation.- 3 percent

### Shock Standoff Distances

Formula.- The formula for shock standoff distance in cm is

$$\delta_C = K_{r,\delta} e^{C_1} \rho_\infty^{C_2+C_3V_\infty} R_B^{C_4+C_5V_\infty} V_\infty^{C_6+C_7V_\infty+C_8V_\infty^2}$$

Derived constants.-

$$K_{r,\delta} = \begin{cases} \dfrac{1}{(0.825784 + 0.14816r)} & (r \neq 1) \\ 1 & (r = 1) \end{cases}$$

| | |
|---|---|
| $C_1 = -3.697$ | $C_5 = -0.01248$ |
| $C_2 = 0.07375$ | $C_6 = 0.7718$ |
| $C_3 = -0.003338$ | $C_7 = -0.02572$ |
| $C_4 = 1.134$ | $C_8 = 0.00009347$ |

Ranges of applicability.-

$\rho_\infty = 1.078 \times 10^{-7}$ to $6.53 \times 10^{-7}$ g/cm$^3$

Altitude = 53.75 to 68.4 km

$R_B$ = 30 to 450 cm

$V_\infty$ = 11 to 16 km/sec

r = 1 to 6

Average deviation.- 2 percent

## REFERENCES


1. Lovelace, Uriel M.: Charts Depicting Kinematic and Heating Parameters for a Ballistic Reentry at Speeds of 26,000 to 45,000 Feet Per Second. NASA TN D-968, 1961.
2. Anderson, John D., Jr.: An Engineering Survey of Radiating Shock Layers. AIAA J., vol. 7, no. 9, Sept. 1969, pp. 1665-1675.
3. Suttles, John T.: A Method of Integral Relations Solution for Radiating, Nonadiabatic, Inviscid Flow Over a Blunt Body. NASA TN D-5480, 1969.
4. Olstad, Walter B.: Blunt-Body Stagnation-Region Flow With Nongray Radiation Heat Transfer – A Singular Perturbation Solution. NASA TR R-295, 1968.
5. Page, William A.; Compton, Dale L.; Borucki, William J.; Ciffone, Donald L.; and Cooper, David M.: Radiative Transport in Inviscid Nonadiabatic Stagnation-Region Shock Layers. AIAA Paper No. 68-784, June 1968.
6. Callis, Linwood B.: Solutions of Blunt-Body Stagnation-Region Flows With Nongray Emission and Absorption of Radiation by a Time-Asymptotic Technique. NASA TR R-299, 1969.
7. Falanga, Ralph A.; and Sullivan, Edward M.: An Inverse-Method Solution for Radiating, Nonadiabatic, Equilibrium Inviscid Flow Over a Blunt Body. NASA TN D-5907, 1970.
8. Garrett, L. Bernard; Smith, G. Louis; and Perkins, John N.: An Implicit Finite-Difference Solution to the Viscous Shock Layer, Including the Effects of Radiation and Strong Blowing. NASA TR R-388, 1972.
9. Olstad, Walter B.: Correlations for Stagnation-Point Radiative Heat Transfer. AIAA J., vol. 7, no. 1, Jan. 1969, pp. 170-172.
10. Wilson, K. H.: RATRAP – A Radiation Transport Code. 6-77-67-12, Lockheed Missiles & Space Co., Mar. 14, 1967.
11. Suttles, John T.: Comparison of the Radiation Flux Profiles and Spectral Detail From Three Detailed Nongray Radiation Models at Conditions Representative of Hypervelocity Earth Entry. NASA TM X-2447, 1972.
12. Sullivan, Edward M.; Erickson, Wayne D.; Smith, G. Louis; and Suttles, John T.: Some Aspects of Interplanetary Earth-Entry Simulation. Paper presented at 15th Annual Meeting of the Institute of Environmental Sciences (Anaheim, Calif.), Apr. 1969.
13. Detra, R. W.; Kemp, N. H.; and Riddell, F. R.: Addendum to 'Heat Transfer to Satellite Vehicles Re-Entering the Atmosphere.' Jet Propulsion, vol. 27, no. 12, Dec. 1957, pp. 1256-1257.

TABLE I.- BASIC DATA

| Case | $V_\infty$, km/sec | Alt., km | $\rho_\infty$, g/cm$^3$ | $R_B$, cm | Axis ratio | $\delta_D$, cm | $q_{R,D}$, W/cm$^2$ | $F_{C,D}$ |
|---|---|---|---|---|---|---|---|---|
| 1 | 11.000 | 58.0 | 3.9072E-07 | 30.00 | 1.0 | 1.421 | 306.0 | - |
| 2 | 11.000 | 58.0 | 3.9072E-07 | 150.00 | 1.0 | 7.036 | 544.0 | - |
| 3 | 11.000 | 58.0 | 3.9072E-07 | 300.00 | 1.0 | 13.974 | 661.0 | - |
| 4 | 11.000 | 58.0 | 3.9072E-07 | 450.00 | 1.0 | 20.844 | 752.0 | - |
| 5 | 13.000 | 58.0 | 3.9072E-07 | 30.00 | 1.0 | 1.368 | 1607.0 | .582 |
| 6 | 13.000 | 58.0 | 3.9072E-07 | 150.00 | 1.0 | 6.680 | 2263.0 | - |
| 7 | 13.000 | 58.0 | 3.9072E-07 | 300.00 | 1.0 | 12.887 | 2699.0 | - |
| 8 | 13.000 | 58.0 | 3.9072E-07 | 450.00 | 1.0 | 18.971 | 3080.0 | - |
| 9 | 14.000 | 58.0 | 3.9072E-07 | 30.00 | 1.0 | 1.339 | 2578.0 | .508 |
| 10 | 14.000 | 58.0 | 3.9072E-07 | 150.00 | 1.0 | 6.374 | 3537.0 | - |
| 11 | 14.000 | 58.0 | 3.9072E-07 | 300.00 | 1.0 | 12.268 | 4289.0 | .307 |
| 12 | 14.000 | 58.0 | 3.9072E-07 | 450.00 | 1.0 | 17.943 | 4816.0 | .285 |
| 13 | 15.000 | 58.0 | 3.9072E-07 | 30.00 | 1.0 | 1.308 | 3709.0 | .452 |
| 14 | 15.000 | 58.0 | 3.9072E-07 | 150.00 | 1.0 | 6.093 | 5124.0 | .298 |
| 15 | 15.000 | 58.0 | 3.9072E-07 | 300.00 | 1.0 | 11.611 | 6108.0 | .268 |
| 16 | 15.000 | 58.0 | 3.9072E-07 | 450.00 | 1.0 | 16.850 | 6917.0 | .252 |
| 17 | 16.000 | 58.0 | 3.9072E-07 | 30.00 | 1.0 | 1.277 | 5462.0 | .401 |
| 18 | 16.000 | 58.0 | 3.9072E-07 | 150.00 | 1.0 | 5.830 | 7039.0 | .261 |
| 19 | 16.000 | 58.0 | 3.9072E-07 | 300.00 | 1.0 | 11.011 | 8176.0 | .231 |
| 20 | 16.000 | 58.0 | 3.9072E-07 | 450.00 | 1.0 | 15.873 | 9382.0 | .224 |
| 21 | 11.000 | 61.0 | 2.7018E-07 | 30.00 | 1.0 | 1.397 | 194.0 | .812 |
| 22 | 11.000 | 61.0 | 2.7018E-07 | 150.00 | 1.0 | 6.921 | 365.0 | .626 |
| 23 | 11.000 | 61.0 | 2.7018E-07 | 300.00 | 1.0 | 13.725 | 447.0 | .541 |
| 24 | 11.000 | 61.0 | 2.7018E-07 | 450.00 | 1.0 | 20.464 | 509.0 | .509 |
| 25 | 12.000 | 61.0 | 2.7018E-07 | 30.00 | 1.0 | 1.378 | 520.0 | .710 |
| 26 | 12.000 | 61.0 | 2.7018E-07 | 150.00 | 1.0 | 6.760 | 843.0 | .497 |
| 27 | 12.000 | 61.0 | 2.7018E-07 | 300.00 | 1.0 | 13.390 | 958.0 | .412 |
| 28 | 12.000 | 61.0 | 2.7018E-07 | 450.00 | 1.0 | 19.844 | 1087.0 | .383 |
| 29 | 13.000 | 61.0 | 2.7018E-07 | 30.00 | 1.0 | 1.348 | 1027.0 | .630 |
| 30 | 13.000 | 61.0 | 2.7018E-07 | 150.00 | 1.0 | 6.640 | 1545.0 | .429 |
| 31 | 13.000 | 61.0 | 2.7018E-07 | 300.00 | 1.0 | 12.710 | 1786.0 | .361 |
| 32 | 13.000 | 61.0 | 2.7018E-07 | 450.00 | 1.0 | 18.800 | 1951.0 | .327 |
| 33 | 14.000 | 61.0 | 2.7018E-07 | 30.00 | 1.0 | 1.319 | 1737.0 | .566 |
| 34 | 14.000 | 61.0 | 2.7018E-07 | 150.00 | 1.0 | 6.280 | 2353.0 | .356 |
| 35 | 14.000 | 61.0 | 2.7018E-07 | 300.00 | 1.0 | 12.090 | 2839.0 | .318 |
| 36 | 14.000 | 61.0 | 2.7018E-07 | 450.00 | 1.0 | 17.660 | 3243.0 | .303 |
| 37 | 15.000 | 61.0 | 2.7018E-07 | 30.00 | 1.0 | 1.287 | 2656.0 | .514 |
| 38 | 15.000 | 61.0 | 2.7018E-07 | 150.00 | 1.0 | 5.995 | 3471.0 | .314 |
| 39 | 15.000 | 61.0 | 2.7018E-07 | 300.00 | 1.0 | 11.440 | 4154.0 | .282 |
| 40 | 15.000 | 61.0 | 2.7018E-07 | 450.00 | 1.0 | 16.850 | 4690.0 | .268 |

TABLE I.- BASIC DATA – Continued

| Case | $V_\infty$, km/sec | Alt., km | $\rho_\infty$, g/cm$^3$ | $R_B$, cm | Axis ratio | $\delta_D$, cm | $q_{R,D}$, W/cm$^2$ | $F_{C,D}$ |
|---|---|---|---|---|---|---|---|---|
| 41 | 16.000 | 61.0 | 2.7018E-07 | 30.00 | 1.0 | 1.256 | 3778.0 | .466 |
| 42 | 16.000 | 61.0 | 2.7018E-07 | 150.00 | 1.0 | 5.713 | 4771.0 | .272 |
| 43 | 16.000 | 61.0 | 2.7018E-07 | 300.00 | 1.0 | 10.920 | 5362.0 | .233 |
| 44 | 16.000 | 61.0 | 2.7018E-07 | 450.00 | 1.0 | 15.550 | 6174.0 | .227 |
| 45 | 11.000 | 67.0 | 1.2959E-07 | 30.00 | 1.0 | 1.360 | 70.0 | – |
| 46 | 11.000 | 67.0 | 1.2959E-07 | 150.00 | 1.0 | 6.754 | 149.0 | – |
| 47 | 11.000 | 67.0 | 1.2959E-07 | 300.00 | 1.0 | 13.445 | 190.0 | – |
| 48 | 11.000 | 67.0 | 1.2959E-07 | 450.00 | 1.0 | 20.019 | 215.0 | – |
| 49 | 12.000 | 67.0 | 1.2959E-07 | 30.00 | 1.0 | 1.342 | 194.0 | – |
| 50 | 12.000 | 67.0 | 1.2959E-07 | 150.00 | 1.0 | 6.597 | 363.0 | – |
| 51 | 12.000 | 67.0 | 1.2959E-07 | 300.00 | 1.0 | 13.045 | 442.0 | – |
| 52 | 12.000 | 67.0 | 1.2959E-07 | 450.00 | 1.0 | 19.392 | 490.0 | – |
| 53 | 13.000 | 67.0 | 1.2959E-07 | 30.00 | 1.0 | 1.317 | 396.0 | – |
| 54 | 13.000 | 67.0 | 1.2959E-07 | 150.00 | 1.0 | 6.392 | 674.0 | – |
| 55 | 13.000 | 67.0 | 1.2959E-07 | 300.00 | 1.0 | 12.525 | 796.0 | – |
| 56 | 13.000 | 67.0 | 1.2959E-07 | 450.00 | 1.0 | 18.498 | 860.0 | – |
| 57 | 14.000 | 67.0 | 1.2959E-07 | 30.00 | 1.0 | 1.292 | 688.0 | – |
| 58 | 14.000 | 67.0 | 1.2959E-07 | 150.00 | 1.0 | 6.194 | 1079.0 | – |
| 59 | 14.000 | 67.0 | 1.2959E-07 | 300.00 | 1.0 | 12.022 | 1218.0 | – |
| 60 | 14.000 | 67.0 | 1.2959E-07 | 450.00 | 1.0 | 17.636 | 1347.0 | – |
| 61 | 15.000 | 67.0 | 1.2959E-07 | 30.00 | 1.0 | 1.268 | 1064.0 | .620 |
| 62 | 15.000 | 67.0 | 1.2959E-07 | 150.00 | 1.0 | 5.980 | 1576.0 | .362 |
| 63 | 15.000 | 67.0 | 1.2959E-07 | 300.00 | 1.0 | 11.470 | 1750.0 | .291 |
| 64 | 15.000 | 67.0 | 1.2959E-07 | 450.00 | 1.0 | 16.710 | 1913.0 | .269 |
| 65 | 16.000 | 67.0 | 1.2959E-07 | 30.00 | 1.0 | 1.242 | 1531.0 | – |
| 66 | 16.000 | 67.0 | 1.2959E-07 | 150.00 | 1.0 | 5.756 | 2150.0 | – |
| 67 | 16.000 | 67.0 | 1.2959E-07 | 300.00 | 1.0 | 10.920 | 2360.0 | – |
| 68 | 16.000 | 67.0 | 1.2959E-07 | 450.00 | 1.0 | 14.850 | 2450.0 | – |
| 69 | 13.000 | 55.0 | 5.6080E-07 | 30.00 | 1.0 | 1.394 | 2388.0 | – |
| 70 | 13.000 | 55.0 | 5.6080E-07 | 150.00 | 1.0 | 6.725 | 3411.0 | – |
| 71 | 13.000 | 55.0 | 5.6080E-07 | 300.00 | 1.0 | 13.064 | 4156.0 | – |
| 72 | 13.000 | 55.0 | 5.6080E-07 | 450.00 | 1.0 | 19.194 | 4752.0 | – |
| 73 | 15.000 | 55.0 | 5.6080E-07 | 30.00 | 1.0 | 1.332 | 5851.0 | – |
| 74 | 15.000 | 55.0 | 5.6080E-07 | 150.00 | 1.0 | 6.209 | 7632.0 | .291 |
| 75 | 15.000 | 55.0 | 5.6080E-07 | 300.00 | 1.0 | 11.770 | 9381.0 | .268 |
| 76 | 15.000 | 55.0 | 5.6080E-07 | 450.00 | 1.0 | 17.040 | 10877.0 | .255 |
| 77 | 16.000 | 55.0 | 5.6080E-07 | 30.00 | 1.0 | 1.298 | 8247.0 | – |
| 78 | 16.000 | 55.0 | 5.6080E-07 | 150.00 | 1.0 | 5.895 | 10294.0 | – |
| 79 | 16.000 | 55.0 | 5.6080E-07 | 300.00 | 1.0 | 11.070 | 12360.0 | – |
| 80 | 16.000 | 55.0 | 5.6080E-07 | 450.00 | 1.0 | 15.918 | 14314.0 | – |

TABLE I.- BASIC DATA – Continued

| Case | $V_\infty$, km/sec | Alt., km | $\rho_\infty$, g/cm3 | $R_B$, cm | Axis ratio | $\delta_D$, cm | $q_{R,D}$, W/cm2 | $F_{C,D}$ |
|---|---|---|---|---|---|---|---|---|
| 81 | 15.025 | 68.3 | 1.0780E-07 | 342.70 | 1.0 | 12.978 | 1542.0 | - |
| 82 | 14.897 | 66.3 | 1.4270E-07 | 342.70 | 1.0 | 13.040 | 2036.0 | - |
| 83 | 14.737 | 64.7 | 1.7580E-07 | 342.70 | 1.0 | 13.243 | 2348.0 | - |
| 84 | 14.549 | 63.4 | 2.0170E-07 | 342.70 | 1.0 | 13.383 | 2616.0 | - |
| 85 | 14.346 | 62.9 | 2.1600E-C7 | 342.70 | 1.0 | 13.535 | 2618.0 | - |
| 86 | 14.161 | 62.8 | 2.1680E-07 | 342.70 | 1.0 | 13.669 | 2435.0 | - |
| 87 | 13.560 | 62.8 | 2.1680E-07 | 342.70 | 1.0 | 14.068 | 1892.0 | - |
| 88 | 13.650 | 63.5 | 2.0259E-07 | 60.96 | 1.0 | 2.634 | 1210.0 | - |
| 89 | 13.169 | 59.3 | 3.3412E-C7 | 60.96 | 1.0 | 2.716 | 1732.0 | - |
| 90 | 12.845 | 57.4 | 4.2147E-07 | 60.96 | 1.0 | 2.766 | 1883.0 | - |
| 91 | 12.009 | 53.7 | 6.5255E-C7 | 60.96 | 1.0 | 2.904 | 1771.0 | - |
| 92 | 15.000 | 59.5 | 3.2535E-07 | 150.00 | 1.0 | 6.079 | 4187.0 | .304 |
| 93 | 15.000 | 59.5 | 3.2535E-C7 | 3C0.00 | 1.0 | 11.608 | 4936.0 | .268 |
| 94 | 15.000 | 59.5 | 3.2535E-07 | 450.00 | 1.0 | 16.870 | 5531.0 | .252 |
| 95 | 15.000 | 64.0 | 1.8837E-07 | 150.00 | 1.0 | 6.015 | 2311.0 | .328 |
| 96 | 15.000 | 64.0 | 1.8837E-07 | 300.00 | 1.0 | 11.530 | 2582.0 | .272 |
| 97 | 15.000 | 64.0 | 1.8837E-07 | 450.00 | 1.0 | 16.625 | 2854.0 | .253 |
| 98 | 15.000 | 70.0 | 8.7535E-08 | 30.00 | 1.0 | 1.258 | 635.0 | .692 |
| 99 | 15.000 | 70.0 | 8.7535E-08 | 150.00 | 1.0 | 5.944 | 1031.0 | .413 |
| 100 | 15.000 | 70.0 | 8.7535E-08 | 300.00 | 1.0 | 11.468 | 1169.0 | .324 |
| 101 | 15.000 | 70.0 | 8.7535E-C8 | 450.00 | 1.0 | 16.599 | 1252.0 | .289 |
| 102 | 13.650 | 63.5 | 2.0259E-07 | 121.92 | 2.0 | 4.688 | 1514.0 | - |
| 103 | 13.169 | 59.3 | 3.3412E-07 | 121.92 | 2.0 | 4.843 | 2090.0 | - |
| 104 | 12.845 | 57.4 | 4.2147E-07 | 121.92 | 2.0 | 4.934 | 2230.0 | - |
| 105 | 12.458 | 55.5 | 5.2997E-C7 | 121.92 | 2.0 | 5.044 | 2236.0 | - |
| 106 | 12.009 | 53.7 | 6.5255E-07 | 121.92 | 2.0 | 5.173 | 2092.0 | - |
| 107 | 11.499 | 52.0 | 8.0413E-07 | 121.92 | 2.0 | 5.290 | 1723.0 | - |
| 108 | 13.650 | 63.5 | 2.0259E-07 | 243.84 | 4.0 | 7.268 | 1639.0 | - |
| 109 | 13.169 | 59.3 | 3.3412E-C7 | 243.84 | 4.0 | 7.501 | 2210.0 | - |
| 110 | 12.845 | 57.4 | 4.2147E-07 | 243.84 | 4.0 | 7.625 | 2419.0 | - |
| 111 | 12.458 | 55.5 | 5.2997E-07 | 243.84 | 4.0 | 7.783 | 2480.0 | - |
| 112 | 12.009 | 53.7 | 6.5255E-07 | 243.84 | 4.0 | 7.978 | 2325.0 | - |
| 113 | 11.499 | 52.0 | 8.0413E-07 | 243.84 | 4.0 | 8.242 | 1966.0 | - |
| 114 | 13.650 | 63.5 | 2.0259E-07 | 365.76 | 6.0 | 8.728 | 1720.0 | - |
| 115 | 13.169 | 59.3 | 3.3412E-07 | 365.76 | 6.0 | 8.963 | 2331.0 | - |
| 116 | 12.845 | 57.4 | 4.2147E-07 | 365.76 | 6.0 | 9.178 | 2553.0 | - |
| 117 | 12.458 | 55.5 | 5.2997E-07 | 365.76 | 6.0 | 9.352 | 2628.0 | - |
| 118 | 12.009 | 53.7 | 6.5255E-07 | 365.76 | 6.0 | 9.575 | 2512.0 | - |
| 119 | 11.499 | 52.0 | 8.0413E-07 | 365.76 | 6.0 | 9.800 | 2263.0 | - |
| 120 | 13.580 | 64.2 | 1.8447E-07 | 243.70 | 4.0 | 6.994 | 1375.0 | - |

TABLE I.- BASIC DATA – Concluded

| Case | $V_\infty$, km/sec | Alt., km | $\rho_\infty$, g/cm3 | $R_B$, cm | Axis ratio | $\delta_D$, cm | $q_{R,D}$, W/cm2 | $F_{C,D}$ |
|---|---|---|---|---|---|---|---|---|
| 121 | 13.232 | 60.1 | 3.0232E-C7 | 243.70 | 4.0 | 7.195 | 2041.0 | - |
| 122 | 12.701 | 56.2 | 4.8433E-07 | 243.70 | 4.0 | 7.423 | 2570.0 | - |
| 123 | 11.949 | 52.6 | 7.4351E-C7 | 243.70 | 4.0 | 7.791 | 2565.0 | - |
| 124 | 10.963 | 49.3 | 1.1199E-06 | 243.70 | 4.0 | 8.134 | 1612.0 | - |
| 125 | 12.700 | 59.2 | 3.3958E-07 | 179.83 | 4.C | 5.644 | 1650.0 | - |
| 126 | 12.254 | 55.4 | 5.3436E-07 | 179.83 | 4.0 | 5.817 | 2049.0 | - |
| 127 | 11.611 | 51.9 | 8.1349E-07 | 179.83 | 4.0 | 6.063 | 1994.0 | - |
| 128 | 13.161 | 61.0 | 2.6849E-07 | 231.64 | 4.0 | 7.094 | 1800.0 | - |
| 129 | 12.767 | 57.1 | 4.3343E-C7 | 231.64 | 4.0 | 7.37C | 2365.0 | - |
| 130 | 12.190 | 53.4 | 6.7347E-07 | 231.64 | 4.0 | 7.545 | 2703.0 | - |
| 131 | 11.398 | 50.0 | 1.0247E-06 | 231.64 | 4.0 | 7.947 | 2339.0 | - |
| 132 | 13.467 | 64.2 | 1.8330E-07 | 262.12 | 4.0 | 7.840 | 1327.0 | - |
| 133 | 12.909 | 59.2 | 3.3693E-07 | 262.12 | 4.0 | 8.073 | 1964.0 | - |
| 134 | 12.220 | 55.5 | 5.2983E-07 | 262.12 | 4.0 | 8.408 | 2168.0 | - |
| 135 | 11.295 | 52.0 | 7.9770E-07 | 262.12 | 4.0 | 8.847 | 1635.0 | - |
| 136 | 13.050 | 61.1 | 2.6667E-07 | 252.98 | 4.0 | 7.724 | 1652.0 | - |
| 137 | 12.592 | 57.2 | 4.2847E-07 | 252.98 | 4.0 | 8.220 | 2169.0 | - |
| 138 | 11.932 | 53.6 | 6.6135E-07 | 252.98 | 4.0 | 8.336 | 2255.0 | - |
| 139 | 11.052 | 50.3 | 9.9419E-07 | 252.98 | 4.0 | 8.695 | 1607.0 | - |
| 140 | 12.700 | 59.2 | 3.3938E-07 | 249.94 | 4.0 | 7.788 | 1763.0 | - |
| 141 | 12.254 | 55.4 | 5.3436E-07 | 249.94 | 4.0 | 8.013 | 2219.0 | - |
| 142 | 11.611 | 51.9 | 8.1349E-07 | 249.94 | 4.0 | 8.396 | 2206.0 | - |
| 143 | 13.016 | 62.0 | 2.3774E-C7 | 231.64 | 4.0 | 7.075 | 1374.0 | - |
| 144 | 12.723 | 58.1 | 3.8424E-07 | 231.64 | 4.0 | 7.276 | 2009.0 | - |
| 145 | 12.281 | 54.4 | 6.0208E-07 | 231.64 | 4.0 | 7.484 | 2534.0 | - |
| 146 | 11.656 | 50.9 | 9.2060E-07 | 231.64 | 4.0 | 7.845 | 2589.0 | - |
| 147 | 10.819 | 47.6 | 1.3803E-06 | 231.64 | 4.0 | 8.238 | 1719.0 | - |
| 148 | 12.909 | 59.2 | 3.3693E-07 | 179.83 | 4.0 | 5.594 | 1829.0 | - |
| 149 | 12.220 | 55.5 | 5.2983E-C7 | 179.83 | 4.0 | 5.820 | 1976.0 | - |
| 150 | 11.931 | 56.6 | 4.6395E-07 | 219.46 | 4.0 | 7.114 | 1444.0 | - |

TABLE II.- MATRIX ELEMENTS AND CONSTANT VECTOR FOR HEATING-RATE CURVE FIT

(a) Matrix elements $a_{ji}$

| j \ i | 1 | 2 | 3 | 4 | 5 | 6 | 7 | 8 | 9 |
|---|---|---|---|---|---|---|---|---|---|
| 1 | *N | $\sum \ln \rho_\infty$ | $\sum V_\infty \ln \rho_\infty$ | $\sum \ln R_B$ | $\sum V_\infty \ln R_B$ | $\sum V_\infty^2 \ln R_B$ | $\sum \ln V_\infty$ | $\sum V_\infty \ln V_\infty$ | $\sum V_\infty^2 \ln V_\infty$ |
| 2 | | $\sum (\ln \rho_\infty)^2$ | $\sum V_\infty (\ln \rho_\infty)^2$ | $\sum \ln \rho_\infty \ln R_B$ | $\sum V_\infty \ln \rho_\infty \ln R_B$ | $\sum V_\infty^2 \ln \rho_\infty \ln R_B$ | $\sum \ln \rho_\infty \ln V_\infty$ | $\sum V_\infty \ln \rho_\infty \ln V_\infty$ | $\sum V_\infty^2 \ln \rho_\infty \ln V_\infty$ |
| 3 | | | $\sum (V_\infty \ln \rho_\infty)^2$ | $\sum V_\infty \ln \rho_\infty \ln R_B$ | $\sum V_\infty^2 \ln \rho_\infty \ln R_B$ | $\sum V_\infty^3 \ln \rho_\infty \ln R_B$ | $\sum V_\infty \ln \rho_\infty \ln V_\infty$ | $\sum V_\infty^2 \ln \rho_\infty \ln V_\infty$ | $\sum V_\infty^3 \ln \rho_\infty \ln V_\infty$ |
| 4 | | | | $\sum (\ln R_B)^2$ | $\sum V_\infty (\ln R_B)^2$ | $\sum (V_\infty \ln R_B)^2$ | $\sum \ln V_\infty \ln R_B$ | $\sum V_\infty \ln V_\infty \ln R_B$ | $\sum V_\infty^2 \ln V_\infty \ln R_B$ |
| 5 | | | | | $\sum (V_\infty \ln R_B)^2$ | $\sum V_\infty^3 (\ln R_B)^2$ | $\sum V_\infty \ln V_\infty \ln R_B$ | $\sum V_\infty^2 \ln V_\infty \ln R_B$ | $\sum V_\infty^3 \ln V_\infty \ln R_B$ |
| 6 | | | SYMMETRIC $a_{ij} = a_{ji}$ | | | $\sum V_\infty^4 (\ln R_B)^2$ | $\sum V_\infty^2 \ln V_\infty \ln R_B$ | $\sum V_\infty^3 \ln V_\infty \ln R_B$ | $\sum V_\infty^4 \ln V_\infty \ln R_B$ |
| 7 | | | | | | | $\sum (\ln V_\infty)^2$ | $\sum V_\infty (\ln V_\infty)^2$ | $\sum (V_\infty \ln V_\infty)^2$ |
| 8 | | | | | | | | $\sum (V_\infty \ln V_\infty)^2$ | $\sum V_\infty^3 (\ln V_\infty)^2$ |
| 9 | | | | | | | | | $\sum V_\infty^4 (\ln V_\infty)^2$ |

*The symbol N represents the total number of data points, and all summations are from 1 to N; that is, $\sum_{n=1}^{N}$.

(b) Constant vector $D_j$

$$D_j = \begin{Bmatrix} \sum \ln q_{R,D} \\ \sum \left(\ln q_{R,D} \ln \rho_\infty\right) \\ \sum \left(V_\infty \ln q_{R,D} \ln \rho_\infty\right) \\ \sum \left(\ln q_{R,D} \ln R_B\right) \\ \sum \left(V_\infty \ln q_{R,D} \ln R_B\right) \\ \sum \left(V_\infty^2 \ln q_{R,D} \ln R_B\right) \\ \sum \left(\ln q_{R,D} \ln V_\infty\right) \\ \sum \left(V_\infty \ln q_{R,D} \ln V_\infty\right) \\ \sum \left(V_\infty^2 \ln q_{R,D} \ln V_\infty\right) \end{Bmatrix}$$

TABLE III.- COMPARISON OF BASIC DATA AND CURVE-FIT RESULTS FOR HEATING RATE

(a) Spherical bodies

| Case | $V_\infty$, km/sec | Alt., km | $\rho_\infty$, g/cm$^3$ | $R_B$, cm | Axis ratio | $q_{R,D}$, W/cm$^2$ | $q_{R,C}$, W/cm$^2$ | Error, percent |
|---|---|---|---|---|---|---|---|---|
| 1 | 11.000 | 58.0 | 3.9072E-07 | 30.00 | 1.0 | 306.0 | 296.5 | 3.107 |
| 2 | 11.000 | 58.0 | 3.9072E-07 | 150.00 | 1.0 | 544.0 | 532.2 | 2.166 |
| 3 | 11.000 | 58.0 | 3.9072E-07 | 300.00 | 1.0 | 661.0 | 684.7 | -3.589 |
| 4 | 11.000 | 58.0 | 3.9072E-07 | 450.00 | 1.0 | 752.0 | 793.5 | -5.513 |
| 5 | 13.000 | 58.0 | 3.9072E-07 | 30.00 | 1.0 | 1607.0 | 1531.5 | 4.701 |
| 6 | 13.000 | 58.0 | 3.9072E-07 | 150.00 | 1.0 | 2263.0 | 2336.9 | -3.267 |
| 7 | 13.000 | 58.0 | 3.9072E-07 | 300.00 | 1.0 | 2699.0 | 2803.4 | -3.870 |
| 8 | 13.000 | 58.0 | 3.9072E-07 | 450.00 | 1.0 | 3080.0 | 3118.4 | -1.247 |
| 9 | 14.000 | 58.0 | 3.9072E-07 | 30.00 | 1.0 | 2578.0 | 2586.9 | -.347 |
| 10 | 14.000 | 58.0 | 3.9072E-07 | 150.00 | 1.0 | 3537.0 | 3735.5 | -5.611 |
| 11 | 14.000 | 58.0 | 3.9072E-07 | 300.00 | 1.0 | 4289.0 | 4375.8 | -2.025 |
| 12 | 14.000 | 58.0 | 3.9072E-07 | 450.00 | 1.0 | 4816.0 | 4800.2 | .328 |
| 13 | 15.000 | 58.0 | 3.9072E-07 | 30.00 | 1.0 | 3709.0 | 3875.3 | -4.484 |
| 14 | 15.000 | 58.0 | 3.9072E-07 | 150.00 | 1.0 | 5124.0 | 5387.7 | -5.146 |
| 15 | 15.000 | 58.0 | 3.9072E-07 | 300.00 | 1.0 | 6108.0 | 6209.1 | -1.656 |
| 16 | 15.000 | 58.0 | 3.9072E-07 | 450.00 | 1.0 | 6917.0 | 6746.6 | 2.464 |
| 17 | 16.000 | 58.0 | 3.9072E-07 | 30.00 | 1.0 | 5462.0 | 5387.4 | 1.365 |
| 18 | 16.000 | 58.0 | 3.9072E-07 | 150.00 | 1.0 | 7039.0 | 7337.3 | -4.238 |
| 19 | 16.000 | 58.0 | 3.9072E-07 | 300.00 | 1.0 | 8176.0 | 8381.4 | -2.512 |
| 20 | 16.000 | 58.0 | 3.9072E-07 | 450.00 | 1.0 | 9382.0 | 9059.7 | 3.435 |
| 21 | 11.000 | 61.0 | 2.7018E-07 | 30.00 | 1.0 | 194.0 | 191.5 | 1.307 |
| 22 | 11.000 | 61.0 | 2.7018E-07 | 150.00 | 1.0 | 365.0 | 343.7 | 5.839 |
| 23 | 11.000 | 61.0 | 2.7018E-07 | 300.00 | 1.0 | 447.0 | 442.2 | 1.081 |
| 24 | 11.000 | 61.0 | 2.7018E-07 | 450.00 | 1.0 | 509.0 | 512.4 | -.665 |
| 25 | 12.000 | 61.0 | 2.7018E-07 | 30.00 | 1.0 | 520.0 | 493.6 | 5.076 |
| 26 | 12.000 | 61.0 | 2.7018E-07 | 150.00 | 1.0 | 843.0 | 809.9 | 3.927 |
| 27 | 12.000 | 61.0 | 2.7018E-07 | 300.00 | 1.0 | 958.0 | 1002.4 | -4.635 |
| 28 | 12.000 | 61.0 | 2.7018E-07 | 450.00 | 1.0 | 1087.0 | 1135.6 | -4.470 |
| 29 | 13.000 | 61.0 | 2.7018E-07 | 30.00 | 1.0 | 1027.0 | 997.9 | 2.832 |

TABLE III.- COMPARISON OF BASIC DATA AND CURVE-FIT RESULTS FOR HEATING RATE – Continued

(a) Spherical bodies – Continued

| Case | $V_\infty$, km/sec | Alt., km | $\rho_\infty$, g/cm$^3$ | $R_B$, cm | Axis ratio | $q_{R,D}$, W/cm$^2$ | $q_{R,C}$, W/cm$^2$ | Error, percent |
|---|---|---|---|---|---|---|---|---|
| 30 | 13.000 | 61.0 | 2.7018E-07 | 150.00 | 1.0 | 1545.0 | 1522.8 | 1.438 |
| 31 | 13.000 | 61.0 | 2.7018E-07 | 300.00 | 1.0 | 1786.0 | 1826.8 | -2.283 |
| 32 | 13.000 | 61.0 | 2.7018E-07 | 450.00 | 1.0 | 1951.0 | 2032.0 | -4.152 |
| 33 | 14.000 | 61.0 | 2.7018E-07 | 30.00 | 1.0 | 1737.0 | 1693.3 | 2.515 |
| 34 | 14.000 | 61.0 | 2.7018E-07 | 150.00 | 1.0 | 2353.0 | 2445.1 | -3.914 |
| 35 | 14.000 | 61.0 | 2.7018E-07 | 300.00 | 1.0 | 2839.0 | 2864.3 | -.890 |
| 36 | 14.000 | 61.0 | 2.7018E-07 | 450.00 | 1.0 | 3243.0 | 3142.0 | 3.113 |
| 37 | 15.000 | 61.0 | 2.7018E-07 | 30.00 | 1.0 | 2656.0 | 2548.1 | 4.062 |
| 38 | 15.000 | 61.0 | 2.7018E-07 | 150.00 | 1.0 | 3471.0 | 3542.5 | -2.061 |
| 39 | 15.000 | 61.0 | 2.7018E-07 | 300.00 | 1.0 | 4154.0 | 4082.7 | 1.718 |
| 40 | 15.000 | 61.0 | 2.7018E-07 | 450.00 | 1.0 | 4690.0 | 4436.0 | 5.416 |
| 41 | 16.000 | 61.0 | 2.7018E-07 | 30.00 | 1.0 | 3778.0 | 3558.4 | 5.814 |
| 42 | 16.000 | 61.0 | 2.7018E-07 | 150.00 | 1.0 | 4771.0 | 4846.3 | -1.578 |
| 43 | 16.000 | 61.0 | 2.7018E-07 | 300.00 | 1.0 | 5362.0 | 5535.9 | -3.243 |
| 44 | 16.000 | 61.0 | 2.7018E-07 | 450.00 | 1.0 | 6174.0 | 5983.9 | 3.079 |
| 45 | 11.000 | 67.0 | 1.2959E-07 | 30.00 | 1.0 | 70.0 | 80.1 | -14.480 |
| 46 | 11.000 | 67.0 | 1.2959E-07 | 150.00 | 1.0 | 149.0 | 143.8 | 3.458 |
| 47 | 11.000 | 67.0 | 1.2959E-07 | 300.00 | 1.0 | 190.0 | 185.1 | 2.597 |
| 48 | 11.000 | 67.0 | 1.2959E-07 | 450.00 | 1.0 | 215.0 | 214.5 | .253 |
| 49 | 12.000 | 67.0 | 1.2959E-07 | 30.00 | 1.0 | 194.0 | 208.5 | -7.453 |
| 50 | 12.000 | 67.0 | 1.2959E-07 | 150.00 | 1.0 | 363.0 | 342.0 | 5.776 |
| 51 | 12.000 | 67.0 | 1.2959E-07 | 300.00 | 1.0 | 442.0 | 423.3 | 4.223 |
| 52 | 12.000 | 67.0 | 1.2959E-07 | 450.00 | 1.0 | 490.0 | 479.6 | 2.127 |
| 53 | 13.000 | 67.0 | 1.2959E-07 | 30.00 | 1.0 | 396.0 | 425.2 | -7.385 |
| 54 | 13.000 | 67.0 | 1.2959E-07 | 150.00 | 1.0 | 674.0 | 648.9 | 3.724 |
| 55 | 13.000 | 67.0 | 1.2959E-07 | 300.00 | 1.0 | 796.0 | 778.4 | 2.206 |
| 56 | 13.000 | 67.0 | 1.2959E-07 | 450.00 | 1.0 | 860.0 | 865.9 | -.686 |
| 57 | 14.000 | 67.0 | 1.2959E-07 | 30.00 | 1.0 | 688.0 | 728.1 | -5.826 |
| 58 | 14.000 | 67.0 | 1.2959E-07 | 150.00 | 1.0 | 1079.0 | 1051.3 | 2.564 |
| 59 | 14.000 | 67.0 | 1.2959E-07 | 300.00 | 1.0 | 1218.0 | 1231.6 | -1.114 |

TABLE III.- COMPARISON OF BASIC DATA AND CURVE-FIT RESULTS FOR HEATING RATE – Continued

(a) Spherical bodies – Concluded

| Case | $V_\infty$, km/sec | Alt., km | $\rho_\infty$, g/cm$^3$ | $R_B$, cm | Axis ratio | $q_{R,D}$, W/cm$^2$ | $q_{R,C}$, W/cm$^2$ | Error, percent |
|---|---|---|---|---|---|---|---|---|
| 60 | 14.000 | 67.0 | 1.2959E-07 | 450.00 | 1.0 | 1347.0 | 1351.0 | -.297 |
| 61 | 15.000 | 67.0 | 1.2959E-07 | 30.00 | 1.0 | 1064.0 | 1105.5 | -3.902 |
| 62 | 15.000 | 67.0 | 1.2959E-07 | 150.00 | 1.0 | 1576.0 | 1537.0 | 2.477 |
| 63 | 15.000 | 67.0 | 1.2959E-07 | 300.00 | 1.0 | 1750.0 | 1771.3 | -1.217 |
| 64 | 15.000 | 67.0 | 1.2959E-07 | 450.00 | 1.0 | 1913.0 | 1924.6 | -.606 |
| 65 | 16.000 | 67.0 | 1.2959E-07 | 30.00 | 1.0 | 1531.0 | 1557.8 | -1.748 |
| 66 | 16.000 | 67.0 | 1.2959E-07 | 150.00 | 1.0 | 2150.0 | 2121.6 | 1.322 |
| 67 | 16.000 | 67.0 | 1.2959E-07 | 300.00 | 1.0 | 2360.0 | 2423.5 | -2.689 |
| 68 | 16.000 | 67.0 | 1.2959E-07 | 450.00 | 1.0 | 2450.0 | 2619.6 | -6.922 |
| 69 | 13.000 | 55.0 | 5.6080E-07 | 30.00 | 1.0 | 2388.0 | 2329.8 | 2.438 |
| 70 | 13.000 | 55.0 | 5.6080E-07 | 150.00 | 1.0 | 3411.0 | 3555.1 | -4.226 |
| 71 | 13.000 | 55.0 | 5.6080E-07 | 300.00 | 1.0 | 4156.0 | 4264.9 | -2.619 |
| 72 | 13.000 | 55.0 | 5.6080E-07 | 450.00 | 1.0 | 4752.0 | 4744.0 | .169 |
| 73 | 15.000 | 55.0 | 5.6080E-07 | 30.00 | 1.0 | 5851.0 | 5843.6 | .127 |
| 74 | 15.000 | 55.0 | 5.6080E-07 | 150.00 | 1.0 | 7632.0 | 8124.1 | -6.448 |
| 75 | 15.000 | 55.0 | 5.6080E-07 | 300.00 | 1.0 | 9381.0 | 9362.8 | .194 |
| 76 | 15.000 | 55.0 | 5.6080E-07 | 450.00 | 1.0 | 10877.0 | 10173.1 | 6.471 |
| 77 | 16.000 | 55.0 | 5.6080E-07 | 30.00 | 1.0 | 8247.0 | 8087.9 | 1.930 |
| 78 | 16.000 | 55.0 | 5.6080E-07 | 150.00 | 1.0 | 10294.0 | 11015.2 | -7.006 |
| 79 | 16.000 | 55.0 | 5.6080E-07 | 300.00 | 1.0 | 12360.0 | 12582.6 | -1.801 |
| 80 | 16.000 | 55.0 | 5.6080E-07 | 450.00 | 1.0 | 14314.0 | 13600.9 | 4.982 |
| 81 | 15.025 | 68.3 | 1.0780E-07 | 342.70 | 1.0 | 1542.0 | 1488.8 | 3.449 |
| 82 | 14.897 | 66.3 | 1.4270E-07 | 342.70 | 1.0 | 2036.0 | 1962.9 | 3.589 |
| 83 | 14.737 | 64.7 | 1.7580E-07 | 342.70 | 1.0 | 2348.0 | 2358.9 | -.465 |
| 84 | 14.549 | 63.4 | 2.0170E-07 | 342.70 | 1.0 | 2616.0 | 2586.4 | 1.133 |
| 85 | 14.346 | 62.9 | 2.1600E-07 | 342.70 | 1.0 | 2618.0 | 2601.8 | .617 |
| 86 | 14.161 | 62.8 | 2.1680E-07 | 342.70 | 1.0 | 2435.0 | 2439.7 | -.193 |
| 87 | 13.560 | 62.8 | 2.1680E-07 | 342.70 | 1.0 | 1892.0 | 1910.4 | -.974 |
| 88 | 13.650 | 63.5 | 2.0259E-07 | 60.96 | 1.0 | 1210.0 | 1215.8 | -.479 |
| 89 | 13.169 | 59.3 | 3.3412E-07 | 60.96 | 1.0 | 1732.0 | 1691.5 | 2.336 |
| 90 | 12.845 | 57.4 | 4.2147E-07 | 60.96 | 1.0 | 1883.0 | 1839.6 | 2.304 |
| 91 | 12.009 | 53.7 | 6.5255E-07 | 60.96 | 1.0 | 1771.0 | 1739.5 | 1.781 |

TABLE III.- COMPARISON OF BASIC DATA AND CURVE-FIT RESULTS FOR HEATING RATE – Continued

(b) Nonspherical bodies

| Case | $V_\infty$, km/sec | Alt., km | $\rho_\infty$, g/cm$^3$ | $R_B$, cm | Axis ratio | $q_{R,D}$, W/cm$^2$ | $q_{R,C}$, W/cm$^2$ | Error, percent |
|---|---|---|---|---|---|---|---|---|
| 102 | 13.650 | 63.5 | 2.0259E-07 | 121.92 | 2.0 | 1514.0 | 1394.8 | 7.874 |
| 103 | 13.169 | 59.3 | 3.3412E-07 | 121.92 | 2.0 | 2090.0 | 1963.6 | 6.050 |
| 104 | 12.845 | 57.4 | 4.2147E-07 | 121.92 | 2.0 | 2230.0 | 2154.5 | 3.385 |
| 105 | 12.458 | 55.5 | 5.2997E-07 | 121.92 | 2.0 | 2236.0 | 2227.8 | .367 |
| 106 | 12.009 | 53.7 | 6.5255E-07 | 121.92 | 2.0 | 2092.0 | 2092.1 | -.004 |
| 107 | 11.499 | 52.0 | 8.0413E-07 | 121.92 | 2.0 | 1723.0 | 1788.6 | -3.810 |
| 108 | 13.650 | 63.5 | 2.0259E-07 | 243.84 | 4.0 | 1639.0 | 1537.2 | 6.209 |
| 109 | 13.169 | 59.3 | 3.3412E-07 | 243.84 | 4.0 | 2210.0 | 2189.7 | .919 |
| 110 | 12.845 | 57.4 | 4.2147E-07 | 243.84 | 4.0 | 2419.0 | 2424.1 | -.212 |
| 111 | 12.458 | 55.5 | 5.2997E-07 | 243.84 | 4.0 | 2480.0 | 2536.0 | -2.256 |
| 112 | 12.009 | 53.7 | 6.5255E-07 | 243.84 | 4.0 | 2325.0 | 2417.3 | -3.968 |
| 113 | 11.499 | 52.0 | 8.0413E-07 | 243.84 | 4.0 | 1966.0 | 2105.8 | -7.112 |
| 114 | 13.650 | 63.5 | 2.0259E-07 | 365.76 | 6.0 | 1720.0 | 1588.6 | 7.640 |
| 115 | 13.169 | 59.3 | 3.3412E-07 | 365.76 | 6.0 | 2331.0 | 2278.5 | 2.254 |
| 116 | 12.845 | 57.4 | 4.2147E-07 | 365.76 | 6.0 | 2553.0 | 2535.6 | .683 |
| 117 | 12.458 | 55.5 | 5.2997E-07 | 365.76 | 6.0 | 2628.0 | 2670.7 | -1.624 |
| 118 | 12.009 | 53.7 | 6.5255E-07 | 365.76 | 6.0 | 2512.0 | 2568.0 | -2.229 |
| 119 | 11.499 | 52.0 | 8.0413E-07 | 365.76 | 6.0 | 2263.0 | 2261.8 | .052 |
| 120 | 13.580 | 64.2 | 1.8447E-07 | 243.70 | 4.0 | 1375.0 | 1337.3 | 2.745 |
| 121 | 13.232 | 60.1 | 3.0232E-07 | 243.70 | 4.0 | 2041.0 | 2011.2 | 1.460 |
| 122 | 12.701 | 56.2 | 4.8433E-07 | 243.70 | 4.0 | 2570.0 | 2631.3 | -2.387 |
| 123 | 11.949 | 52.6 | 7.4351E-07 | 243.70 | 4.0 | 2565.0 | 2700.9 | -5.298 |
| 124 | 10.963 | 49.3 | 1.1199E-06 | 243.70 | 4.0 | 1612.0 | 1938.4 | -20.250 |
| 125 | 12.700 | 59.2 | 3.3958E-07 | 179.83 | 4.0 | 1650.0 | 1599.7 | 3.047 |

TABLE III.- COMPARISON OF BASIC DATA AND CURVE-FIT RESULTS FOR HEATING RATE – Concluded

(b) Nonspherical bodies – Concluded

| Case | $V_\infty$, km/sec | Alt., km | $\rho_\infty$, g/cm$^3$ | $R_B$, cm | Axis ratio | $q_{R,D}$, W/cm$^2$ | $q_{R,C}$, W/cm$^2$ | Error, percent |
|---|---|---|---|---|---|---|---|---|
| 126 | 12.254 | 55.4 | 5.3436E-07 | 179.83 | 4.0 | 2049.0 | 2060.0 | -.536 |
| 127 | 11.611 | 51.9 | 8.1349E-07 | 179.83 | 4.0 | 1994.0 | 2112.6 | -5.949 |
| 128 | 13.161 | 61.0 | 2.6849E-07 | 231.64 | 4.0 | 1800.0 | 1670.6 | 7.190 |
| 129 | 12.767 | 57.1 | 4.3343E-07 | 231.64 | 4.0 | 2365.0 | 2366.3 | -.053 |
| 130 | 12.190 | 53.4 | 6.7347E-07 | 231.64 | 4.0 | 2703.0 | 2791.2 | -3.262 |
| 131 | 11.398 | 50.0 | 1.0247E-06 | 231.64 | 4.0 | 2339.0 | 2534.5 | -8.356 |
| 132 | 13.467 | 64.2 | 1.8330E-07 | 262.12 | 4.0 | 1327.0 | 1283.5 | 3.281 |
| 133 | 12.909 | 59.2 | 3.3693E-07 | 262.12 | 4.0 | 1964.0 | 1971.7 | -.393 |
| 134 | 12.220 | 55.5 | 5.2983E-07 | 262.12 | 4.0 | 2168.0 | 2230.0 | -2.860 |
| 135 | 11.295 | 52.0 | 7.9770E-07 | 262.12 | 4.0 | 1635.0 | 1801.8 | -10.200 |
| 136 | 13.050 | 61.1 | 2.6667E-07 | 252.98 | 4.0 | 1652.0 | 1602.7 | 2.984 |
| 137 | 12.592 | 57.2 | 4.2847E-07 | 252.98 | 4.0 | 2169.0 | 2165.3 | .171 |
| 138 | 11.932 | 53.6 | 6.6135E-07 | 252.98 | 4.0 | 2255.0 | 2353.0 | -4.345 |
| 139 | 11.052 | 50.3 | 9.9419E-07 | 252.98 | 4.0 | 1607.0 | 1856.3 | -15.511 |
| 140 | 12.700 | 59.2 | 3.3938E-07 | 249.94 | 4.0 | 1763.0 | 1750.1 | .732 |
| 141 | 12.254 | 55.4 | 5.3436E-07 | 249.94 | 4.0 | 2219.0 | 2270.2 | -2.308 |
| 142 | 11.611 | 51.9 | 8.1349E-07 | 249.94 | 4.0 | 2206.0 | 2353.6 | -6.691 |
| 143 | 13.016 | 62.0 | 2.3774E-07 | 231.64 | 4.0 | 1374.0 | 1346.8 | 1.980 |
| 144 | 12.723 | 58.1 | 3.8424E-07 | 231.64 | 4.0 | 2009.0 | 2006.5 | .124 |
| 145 | 12.281 | 54.4 | 6.0208E-07 | 231.64 | 4.0 | 2534.0 | 2597.2 | -2.494 |
| 146 | 11.656 | 50.9 | 9.2060E-07 | 231.64 | 4.0 | 2589.0 | 2750.6 | -6.243 |
| 147 | 10.819 | 47.6 | 1.3803E-06 | 231.64 | 4.0 | 1719.0 | 2115.9 | -23.090 |
| 148 | 12.909 | 59.2 | 3.3693E-07 | 179.83 | 4.0 | 1829.0 | 1783.5 | 2.487 |
| 149 | 12.220 | 55.5 | 5.2983E-07 | 179.83 | 4.0 | 1976.0 | 1994.0 | -.913 |
| 150 | 11.931 | 56.6 | 4.6395E-07 | 219.46 | 4.0 | 1444.0 | 1483.7 | -2.749 |

TABLE IV.- MATRIX ELEMENTS AND CONSTANT VECTOR FOR COOLING-FACTOR CURVE FIT

(a) Matrix elements $b_{ji}$

| j \ i | 1 | 2 | 3 | 4 | 5 | 6 | 7 |
|---|---|---|---|---|---|---|---|
| 1 | *N | $\sum \ln \rho_\infty$ | $\sum (R_B \ln \rho_\infty)$ | $\sum (R_B^2 \ln \rho_\infty)$ | $\sum (R_B^3 \ln \rho_\infty)$ | $\sum \ln R_B$ | $\sum \ln V_\infty$ |
| 2 | | $\sum (\ln \rho_\infty)^2$ | $\sum \left[R_B (\ln \rho_\infty)^2\right]$ | $\sum (R_B \ln \rho_\infty)^2$ | $\sum \left[R_B^3 (\ln \rho_\infty)^2\right]$ | $\sum (\ln \rho_\infty \ln R_B)$ | $\sum (\ln \rho_\infty \ln V_\infty)$ |
| 3 | | | $\sum (R_B \ln \rho_\infty)^2$ | $\sum \left[R_B^3 (\ln \rho_\infty)^2\right]$ | $\sum \left[R_B^4 (\ln \rho_\infty)^2\right]$ | $\sum (R_B \ln \rho_\infty \ln R_B)$ | $\sum (R_B \ln \rho_\infty \ln V_\infty)$ |
| 4 | | | | $\sum \left[R_B^4 (\ln \rho_\infty)^2\right]$ | $\sum \left[R_B^5 (\ln \rho_\infty)^2\right]$ | $\sum (R_B^2 \ln \rho_\infty \ln R_B)$ | $\sum (R_B^2 \ln \rho_\infty \ln V_\infty)$ |
| 5 | | | SYMMETRIC $b_{ij} = b_{ji}$ | | $\sum \left[R_B^6 (\ln \rho_\infty)^2\right]$ | $\sum (R_B^3 \ln \rho_\infty \ln R_B)$ | $\sum (R_B^3 \ln \rho_\infty \ln V_\infty)$ |
| 6 | | | | | | $\sum (\ln R_B)^2$ | $\sum (\ln V_\infty \ln R_B)$ |
| 7 | | | | | | | $\sum (\ln V_\infty)^2$ |

*The symbol N represents the total number of data points, and all summations are from 1 to N; that is, $\sum_{n=1}^{N}$.

(b) Constant vector $G_j$

$$G_j = \begin{Bmatrix} \sum \ln F_{C,D} \\ \sum (\ln F_{C,D} \ln \rho_\infty) \\ \sum (R_B \ln F_{C,D} \ln \rho_\infty) \\ \sum (R_B^2 \ln F_{C,D} \ln \rho_\infty) \\ \sum (R_B^3 \ln F_{C,D} \ln \rho_\infty) \\ \sum (\ln F_{C,D} \ln R_B) \\ \sum (\ln F_{C,D} \ln V_\infty) \end{Bmatrix}$$

TABLE V.- COMPARISON OF BASIC DATA AND CURVE-FIT RESULTS FOR COOLING FACTOR

| Case | $V_\infty$, km/sec | Alt., km | $\rho_\infty$, g/cm$^3$ | $R_B$, cm | Axis ratio | $F_{C,D}$ | $F_{C,C}$ | Error, percent |
|---|---|---|---|---|---|---|---|---|
| 5 | 13.000 | 58.0 | 3.9072E-07 | 30.00 | 1.0 | .582 | .580 | .383 |
| 9 | 14.000 | 58.0 | 3.9072E-07 | 30.00 | 1.0 | .508 | .502 | 1.089 |
| 11 | 14.000 | 58.0 | 3.9072E-07 | 300.00 | 1.0 | .307 | .305 | .800 |
| 12 | 14.000 | 58.0 | 3.9072E-07 | 450.00 | 1.0 | .285 | .290 | -1.636 |
| 13 | 15.000 | 58.0 | 3.9072E-07 | 30.00 | 1.0 | .452 | .440 | 2.700 |
| 14 | 15.000 | 58.0 | 3.9072E-07 | 150.00 | 1.0 | .298 | .302 | -1.432 |
| 15 | 15.000 | 58.0 | 3.9072E-07 | 300.00 | 1.0 | .268 | .267 | .538 |
| 16 | 15.000 | 58.0 | 3.9072E-07 | 450.00 | 1.0 | .252 | .254 | -.608 |
| 17 | 16.000 | 58.0 | 3.9072E-07 | 30.00 | 1.0 | .401 | .388 | 3.176 |
| 18 | 16.000 | 58.0 | 3.9072E-07 | 150.00 | 1.0 | .261 | .267 | -2.241 |
| 19 | 16.000 | 58.0 | 3.9072E-07 | 300.00 | 1.0 | .231 | .235 | -1.872 |
| 20 | 16.000 | 58.0 | 3.9072E-07 | 450.00 | 1.0 | .224 | .224 | .078 |
| 21 | 11.000 | 61.0 | 2.7018E-07 | 30.00 | 1.0 | .812 | .895 | -10.279 |
| 22 | 11.000 | 61.0 | 2.7018E-07 | 150.00 | 1.0 | .626 | .584 | 6.666 |
| 23 | 11.000 | 61.0 | 2.7018E-07 | 300.00 | 1.0 | .541 | .504 | 6.786 |
| 24 | 11.000 | 61.0 | 2.7018E-07 | 450.00 | 1.0 | .509 | .474 | 6.890 |
| 25 | 12.000 | 61.0 | 2.7018E-07 | 30.00 | 1.0 | .710 | .757 | -6.616 |
| 26 | 12.000 | 61.0 | 2.7018E-07 | 150.00 | 1.0 | .497 | .494 | .623 |
| 27 | 12.000 | 61.0 | 2.7018E-07 | 300.00 | 1.0 | .412 | .426 | -3.470 |
| 28 | 12.000 | 61.0 | 2.7018E-07 | 450.00 | 1.0 | .383 | .401 | -4.603 |
| 29 | 13.000 | 61.0 | 2.7018E-07 | 30.00 | 1.0 | .630 | .649 | -2.947 |
| 30 | 13.000 | 61.0 | 2.7018E-07 | 150.00 | 1.0 | .429 | .423 | 1.359 |
| 31 | 13.000 | 61.0 | 2.7018E-07 | 300.00 | 1.0 | .361 | .365 | -1.176 |
| 32 | 13.000 | 61.0 | 2.7018E-07 | 450.00 | 1.0 | .327 | .343 | -4.971 |
| 33 | 14.000 | 61.0 | 2.7018E-07 | 30.00 | 1.0 | .566 | .562 | .691 |
| 34 | 14.000 | 61.0 | 2.7018E-07 | 150.00 | 1.0 | .356 | .367 | -3.019 |

TABLE V.- COMPARISON OF BASIC DATA AND CURVE-FIT RESULTS FOR COOLING FACTOR – Concluded

| Case | $V_\infty$, km/sec | Alt., km | $\rho_\infty$, g/cm3 | $R_B$, cm | Axis ratio | $F_{C,D}$ | $F_{C,C}$ | Error, percent |
|---|---|---|---|---|---|---|---|---|
| 35 | 14.000 | 61.0 | 2.7018E-07 | 300.00 | 1.0 | .318 | .317 | .458 |
| 36 | 14.000 | 61.0 | 2.7018E-07 | 450.00 | 1.0 | .303 | .297 | 1.819 |
| 37 | 15.000 | 61.0 | 2.7018E-07 | 30.00 | 1.0 | .514 | .492 | 4.284 |
| 38 | 15.000 | 61.0 | 2.7018E-07 | 150.00 | 1.0 | .314 | .321 | -2.230 |
| 39 | 15.000 | 61.0 | 2.7018E-07 | 300.00 | 1.0 | .282 | .277 | 1.751 |
| 40 | 15.000 | 61.0 | 2.7018E-07 | 450.00 | 1.0 | .268 | .260 | 2.843 |
| 41 | 16.000 | 61.0 | 2.7018E-07 | 30.00 | 1.0 | .466 | .434 | 6.795 |
| 42 | 16.000 | 61.0 | 2.7018E-07 | 150.00 | 1.0 | .272 | .283 | -4.188 |
| 43 | 16.000 | 61.0 | 2.7018E-07 | 300.00 | 1.0 | .233 | .245 | -4.978 |
| 44 | 16.000 | 61.0 | 2.7018E-07 | 450.00 | 1.0 | .227 | .230 | -1.265 |
| 61 | 15.000 | 67.0 | 1.2959E-07 | 30.00 | 1.0 | .620 | .615 | .793 |
| 62 | 15.000 | 67.0 | 1.2959E-07 | 150.00 | 1.0 | .362 | .362 | .041 |
| 63 | 15.000 | 67.0 | 1.2959E-07 | 300.00 | 1.0 | .291 | .299 | -2.828 |
| 64 | 15.000 | 67.0 | 1.2959E-07 | 450.00 | 1.0 | .269 | .275 | -2.074 |
| 74 | 15.000 | 55.0 | 5.6080E-07 | 150.00 | 1.0 | .291 | .285 | 2.071 |
| 75 | 15.000 | 55.0 | 5.6080E-07 | 300.00 | 1.0 | .268 | .257 | 4.233 |
| 76 | 15.000 | 55.0 | 5.6080E-07 | 450.00 | 1.0 | .255 | .247 | 3.139 |
| 92 | 15.000 | 59.5 | 3.2535E-07 | 150.00 | 1.0 | .304 | .311 | -2.442 |
| 93 | 15.000 | 59.5 | 3.2535E-07 | 300.00 | 1.0 | .268 | .272 | -1.388 |
| 94 | 15.000 | 59.5 | 3.2535E-07 | 450.00 | 1.0 | .252 | .257 | -1.948 |
| 95 | 15.000 | 64.0 | 1.8837E-07 | 150.00 | 1.0 | .328 | .340 | -3.794 |
| 96 | 15.000 | 64.0 | 1.8837E-07 | 300.00 | 1.0 | .272 | .288 | -5.783 |
| 97 | 15.000 | 64.0 | 1.8837E-07 | 450.00 | 1.0 | .253 | .267 | -5.635 |
| 98 | 15.000 | 70.0 | 8.7535E-08 | 30.00 | 1.0 | .692 | .693 | -.143 |
| 99 | 15.000 | 70.0 | 8.7535E-08 | 150.00 | 1.0 | .413 | .386 | 6.598 |
| 100 | 15.000 | 70.0 | 8.7535E-08 | 300.00 | 1.0 | .324 | .312 | 3.770 |
| 101 | 15.000 | 70.0 | 8.7535E-08 | 450.00 | 1.0 | .289 | .282 | 2.258 |

TABLE VI.- MATRIX ELEMENTS AND CONSTANT VECTOR FOR STANDOFF-DISTANCE CURVE FIT

(a) Matrix elements $c_{ji}$

| j \ i | 1 | 2 | 3 | 4 | 5 | 6 | 7 | 8 |
|---|---|---|---|---|---|---|---|---|
| 1 | *N | $\sum \ln \rho_\infty$ | $\sum (V_\infty \ln \rho_\infty)$ | $\sum \ln R_B$ | $\sum (V_\infty \ln R_B)$ | $\sum \ln V_\infty$ | $\sum (V_\infty \ln V_\infty)$ | $\sum (V_\infty^2 \ln V_\infty)$ |
| 2 | | $\sum (\ln \rho_\infty)^2$ | $\sum \left[V_\infty (\ln \rho_\infty)^2\right]$ | $\sum (\ln \rho_\infty \ln R_B)$ | $\sum (V_\infty \ln \rho_\infty \ln R_B)$ | $\sum (\ln \rho_\infty \ln V_\infty)$ | $\sum (V_\infty \ln \rho_\infty \ln V_\infty)$ | $\sum (V_\infty^2 \ln \rho_\infty \ln V_\infty)$ |
| 3 | | | $\sum \left[V_\infty^2 (\ln \rho_\infty)^2\right]$ | $\sum (V_\infty \ln \rho_\infty \ln R_B)$ | $\sum (V_\infty^2 \ln \rho_\infty \ln R_B)$ | $\sum (V_\infty \ln \rho_\infty \ln V_\infty)$ | $\sum (V_\infty^2 \ln \rho_\infty \ln V_\infty)$ | $\sum (V_\infty^3 \ln \rho_\infty \ln V_\infty)$ |
| 4 | | | | $\sum (\ln R_B)^2$ | $\sum \left[V_\infty (\ln R_B)^2\right]$ | $\sum (\ln V_\infty \ln R_B)$ | $\sum (V_\infty \ln V_\infty \ln R_B)$ | $\sum (V_\infty^2 \ln V_\infty \ln R_B)$ |
| 5 | | | SYMMETRIC | | $\sum \left[V_\infty^2 (\ln R_B)^2\right]$ | $\sum (V_\infty \ln V_\infty \ln R_B)$ | $\sum (V_\infty^2 \ln V_\infty \ln R_B)$ | $\sum (V_\infty^3 \ln V_\infty \ln R_B)$ |
| 6 | | | | $c_{ij} = c_{ji}$ | | $\sum (\ln V_\infty)^2$ | $\sum \left[V_\infty (\ln V_\infty)^2\right]$ | $\sum \left[V_\infty^2 (\ln V_\infty)^2\right]$ |
| 7 | | | | | | | $\sum \left[V_\infty^2 (\ln V_\infty)^2\right]$ | $\sum \left[V_\infty^3 (\ln V_\infty)^2\right]$ |
| 8 | | | | | | | | $\sum \left[V_\infty^4 (\ln V_\infty)^2\right]$ |

*The symbol N represents the total number of data points, and all summations are from 1 to N; that is, $\sum_{n=1}^{N}$

(b) Constant vector $H_j$

$$H_j = \begin{Bmatrix} \sum \ln \delta_D \\ \sum (\ln \delta_D \ln \rho_\infty) \\ \sum (V_\infty \ln \delta_D \ln \rho_\infty) \\ \sum (\ln \delta_D \ln R_B) \\ \sum (V_\infty \ln \delta_D \ln R_B) \\ \sum (\ln \delta_D \ln V_\infty) \\ \sum (V_\infty \ln \delta_D \ln V_\infty) \\ \sum (V_\infty^2 \ln \delta_D \ln V_\infty) \end{Bmatrix}$$

TABLE VII.- COMPARISON OF BASIC DATA AND CURVE-FIT RESULTS

FOR SHOCK STANDOFF DISTANCE

(a) Spherical bodies

| Case | $V_{\infty}$, km/sec | Alt., km | $\rho_{\infty}$, g/cm3 | $R_B$, cm | Axis ratio | $\delta_D$, cm | $\delta_C$, cm | Error, percent |
|---|---|---|---|---|---|---|---|---|
| 1 | 11.000 | 58.0 | 3.9072E-C7 | 30.00 | 1.0 | 1.421 | 1.413 | .532 |
| 2 | 11.000 | 58.0 | 3.9072E-07 | 150.00 | 1.0 | 7.036 | 7.030 | .085 |
| 3 | 11.000 | 58.0 | 3.9072E-C7 | 3C0.00 | 1.0 | 13.974 | 14.028 | -.387 |
| 4 | 11.000 | 58.0 | 3.9072E-C7 | 450.00 | 1.0 | 20.844 | 21.014 | -.816 |
| 5 | 13.000 | 58.0 | 3.9072E-C7 | 30.00 | 1.0 | 1.368 | 1.381 | -.946 |
| 6 | 13.000 | 58.0 | 3.9072E-C7 | 150.0C | 1.0 | 6.680 | 6.598 | 1.229 |
| 7 | 13.000 | 58.0 | 3.9072E-07 | 300.00 | 1.0 | 12.887 | 12.940 | -.411 |
| 8 | 13.000 | 58.0 | 3.9072E-C7 | 450.00 | 1.0 | 18.971 | 19.189 | -1.149 |
| 9 | 14.000 | 58.0 | 3.9072E-07 | 30.00 | 1.0 | 1.339 | 1.352 | -1.007 |
| 10 | 14.000 | 58.0 | 3.9072E-C7 | 150.00 | 1.0 | 6.374 | 6.333 | .636 |
| 11 | 14.000 | 58.0 | 3.9072E-07 | 3C0.00 | 1.0 | 12.268 | 12.314 | -.378 |
| 12 | 14.000 | 58.0 | 3.9072E-C7 | 450.00 | 1.0 | 17.943 | 18.169 | -1.260 |
| 13 | 15.000 | 58.0 | 3.9072E-C7 | 30.00 | 1.0 | 1.308 | 1.318 | -.764 |
| 14 | 15.000 | 58.0 | 3.9072E-07 | 150.00 | 1.0 | 6.093 | 6.049 | .719 |
| 15 | 15.000 | 58.0 | 3.9072E-07 | 300.00 | 1.0 | 11.611 | 11.660 | -.425 |
| 16 | 15.000 | 58.0 | 3.9072E-C7 | 450.00 | 1.0 | 16.850 | 17.117 | -1.586 |
| 17 | 16.000 | 58.0 | 3.9072E-07 | 30.00 | 1.0 | 1.277 | 1.279 | -.139 |
| 18 | 16.000 | 58.0 | 3.9072E-C7 | 150.00 | 1.0 | 5.830 | 5.753 | 1.329 |
| 19 | 16.000 | 58.0 | 3.9072E-07 | 300.00 | 1.0 | 11.011 | 10.993 | .164 |
| 20 | 16.000 | 58.0 | 3.9072E-C7 | 450.00 | 1.0 | 15.873 | 16.056 | -1.154 |
| 21 | 11.000 | 61.0 | 2.7018E-07 | 30.00 | 1.0 | 1.397 | 1.394 | .196 |
| 22 | 11.000 | 61.0 | 2.7018E-07 | 150.00 | 1.0 | 6.921 | 6.935 | -.197 |
| 23 | 11.000 | 61.0 | 2.7018E-C7 | 300.00 | 1.0 | 13.725 | 13.838 | -.821 |
| 24 | 11.000 | 61.0 | 2.7018E-07 | 450.00 | 1.0 | 20.464 | 20.729 | -1.295 |
| 25 | 12.000 | 61.0 | 2.7018E-C7 | 30.00 | 1.0 | 1.378 | 1.385 | -.473 |
| 26 | 12.000 | 61.0 | 2.7018E-07 | 150.00 | 1.0 | 6.760 | 6.749 | .159 |
| 27 | 12.000 | 61.0 | 2.7018E-C7 | 300.00 | 1.0 | 13.390 | 13.352 | .285 |
| 28 | 12.000 | 61.0 | 2.7018E-07 | 450.00 | 1.0 | 19.844 | 19.900 | -.283 |
| 29 | 13.000 | 61.0 | 2.7018E-C7 | 30.00 | 1.0 | 1.348 | 1.366 | -1.303 |

TABLE VII.- COMPARISON OF BASIC DATA AND CURVE-FIT RESULTS

FOR SHOCK STANDOFF DISTANCE – Continued

(a) Spherical bodies – Continued

| Case | $V_\infty$, km/sec | Alt., km | $\rho_\infty$, g/cm3 | $R_B$, cm | Axis ratio | $\delta_D$, cm | $\delta_C$, cm | Error, percent |
|---|---|---|---|---|---|---|---|---|
| 30 | 13.000 | 61.0 | 2.7018E-07 | 150.00 | 1.0 | 6.640 | 6.524 | 1.740 |
| 31 | 13.000 | 61.0 | 2.7018E-07 | 300.00 | 1.0 | 12.710 | 12.796 | -.676 |
| 32 | 13.000 | 61.0 | 2.7018E-07 | 450.00 | 1.0 | 18.800 | 18.975 | -.933 |
| 33 | 14.000 | 61.0 | 2.7018E-07 | 30.00 | 1.0 | 1.319 | 1.339 | -1.522 |
| 34 | 14.000 | 61.0 | 2.7018E-07 | 150.00 | 1.0 | 6.280 | 6.271 | .149 |
| 35 | 14.000 | 61.0 | 2.7018E-07 | 300.00 | 1.0 | 12.090 | 12.192 | -.846 |
| 36 | 14.000 | 61.0 | 2.7018E-07 | 450.00 | 1.0 | 17.660 | 17.989 | -1.862 |
| 37 | 15.000 | 61.0 | 2.7018E-07 | 30.00 | 1.0 | 1.287 | 1.307 | -1.517 |
| 38 | 15.000 | 61.0 | 2.7018E-07 | 150.00 | 1.0 | 5.995 | 5.997 | -.026 |
| 39 | 15.000 | 61.0 | 2.7018E-07 | 300.00 | 1.0 | 11.440 | 11.559 | -1.040 |
| 40 | 15.000 | 61.0 | 2.7018E-07 | 450.00 | 1.0 | 16.850 | 16.968 | -.703 |
| 41 | 16.000 | 61.0 | 2.7018E-07 | 30.00 | 1.0 | 1.256 | 1.269 | -1.053 |
| 42 | 16.000 | 61.0 | 2.7018E-07 | 150.00 | 1.0 | 5.713 | 5.710 | .061 |
| 43 | 16.000 | 61.0 | 2.7018E-07 | 300.00 | 1.0 | 10.920 | 10.911 | .084 |
| 44 | 16.000 | 61.0 | 2.7018E-07 | 450.00 | 1.0 | 15.550 | 15.936 | -2.483 |
| 45 | 11.000 | 67.0 | 1.2959E-07 | 30.00 | 1.0 | 1.360 | 1.357 | .232 |
| 46 | 11.000 | 67.0 | 1.2959E-07 | 150.00 | 1.0 | 6.754 | 6.748 | .082 |
| 47 | 11.000 | 67.0 | 1.2959E-07 | 300.00 | 1.0 | 13.445 | 13.466 | -.158 |
| 48 | 11.000 | 67.0 | 1.2959E-07 | 450.00 | 1.0 | 20.019 | 20.173 | -.767 |
| 49 | 12.000 | 67.0 | 1.2959E-07 | 30.00 | 1.0 | 1.342 | 1.351 | -.646 |
| 50 | 12.000 | 67.0 | 1.2959E-07 | 150.00 | 1.0 | 6.597 | 6.584 | .194 |
| 51 | 12.000 | 67.0 | 1.2959E-07 | 300.00 | 1.0 | 13.045 | 13.025 | .151 |
| 52 | 12.000 | 67.0 | 1.2959E-07 | 450.00 | 1.0 | 19.392 | 19.414 | -.111 |
| 53 | 13.000 | 67.0 | 1.2959E-07 | 30.00 | 1.0 | 1.317 | 1.335 | -1.400 |
| 54 | 13.000 | 67.0 | 1.2959E-07 | 150.00 | 1.0 | 6.392 | 6.381 | .179 |
| 55 | 13.000 | 67.0 | 1.2959E-07 | 300.00 | 1.0 | 12.525 | 12.514 | .090 |
| 56 | 13.000 | 67.0 | 1.2959E-07 | 450.00 | 1.0 | 18.498 | 18.557 | -.318 |
| 57 | 14.000 | 67.0 | 1.2959E-07 | 30.00 | 1.0 | 1.292 | 1.313 | -1.606 |
| 58 | 14.000 | 67.0 | 1.2959E-07 | 150.00 | 1.0 | 6.194 | 6.147 | .753 |
| 59 | 14.000 | 67.0 | 1.2959E-07 | 300.00 | 1.0 | 12.022 | 11.953 | .577 |

## TABLE VII.- COMPARISON OF BASIC DATA AND CURVE-FIT RESULTS FOR SHOCK STANDOFF DISTANCE – Continued

### (a) Spherical bodies – Concluded

| Case | $V_\infty$, km/sec | Alt., km | $\rho_\infty$, g/cm$^3$ | $R_B$, cm | Axis ratio | $\delta_D$, cm | $\delta_C$, cm | Error, percent |
|---|---|---|---|---|---|---|---|---|
| 60 | 14.000 | 67.0 | 1.2959E-07 | 450.00 | 1.0 | 17.636 | 17.635 | .004 |
| 61 | 15.000 | 67.0 | 1.2959E-07 | 30.00 | 1.0 | 1.268 | 1.284 | -1.261 |
| 62 | 15.000 | 67.0 | 1.2959E-07 | 150.00 | 1.0 | 5.980 | 5.893 | 1.452 |
| 63 | 15.000 | 67.0 | 1.2959E-07 | 300.00 | 1.0 | 11.470 | 11.360 | .963 |
| 64 | 15.000 | 67.0 | 1.2959E-07 | 450.00 | 1.0 | 16.710 | 16.676 | .205 |
| 65 | 16.000 | 67.0 | 1.2959E-07 | 30.00 | 1.0 | 1.242 | 1.250 | -.676 |
| 66 | 16.000 | 67.0 | 1.2959E-07 | 150.00 | 1.0 | 5.756 | 5.625 | 2.279 |
| 67 | 16.000 | 67.0 | 1.2959E-07 | 300.00 | 1.0 | 10.920 | 10.749 | 1.566 |
| 68 | 16.000 | 67.0 | 1.2959E-07 | 450.00 | 1.0 | 14.850 | 15.700 | -5.722 |
| 69 | 13.000 | 55.0 | 5.6080E-07 | 30.00 | 1.0 | 1.394 | 1.396 | -.156 |
| 70 | 13.000 | 55.0 | 5.6080E-07 | 150.00 | 1.0 | 6.725 | 6.671 | .808 |
| 71 | 13.000 | 55.0 | 5.6080E-07 | 300.00 | 1.0 | 13.064 | 13.083 | -.144 |
| 72 | 13.000 | 55.0 | 5.6080E-07 | 450.00 | 1.0 | 19.194 | 19.401 | -1.077 |
| 73 | 15.000 | 55.0 | 5.6080E-07 | 30.00 | 1.0 | 1.332 | 1.329 | .201 |
| 74 | 15.000 | 55.0 | 5.6080E-07 | 150.00 | 1.0 | 6.209 | 6.101 | 1.737 |
| 75 | 15.000 | 55.0 | 5.6080E-07 | 300.00 | 1.0 | 11.770 | 11.761 | .080 |
| 76 | 15.000 | 55.0 | 5.6080E-07 | 450.00 | 1.0 | 17.040 | 17.264 | -1.317 |
| 77 | 16.000 | 55.0 | 5.6080E-07 | 30.00 | 1.0 | 1.298 | 1.288 | .754 |
| 78 | 16.000 | 55.0 | 5.6080E-07 | 150.00 | 1.0 | 5.895 | 5.795 | 1.697 |
| 79 | 16.000 | 55.0 | 5.6080E-07 | 300.00 | 1.0 | 11.070 | 11.074 | -.037 |
| 80 | 16.000 | 55.0 | 5.6080E-07 | 450.00 | 1.0 | 15.918 | 16.175 | -1.612 |
| 81 | 15.025 | 68.3 | 1.0780E-07 | 342.70 | 1.0 | 12.978 | 12.811 | 1.283 |
| 82 | 14.897 | 66.3 | 1.4270E-07 | 342.70 | 1.0 | 13.040 | 12.988 | .402 |
| 83 | 14.737 | 64.7 | 1.7580E-07 | 342.70 | 1.0 | 13.243 | 13.168 | .564 |
| 84 | 14.549 | 63.4 | 2.0170E-07 | 342.70 | 1.0 | 13.383 | 13.349 | .251 |
| 85 | 14.346 | 62.9 | 2.1600E-07 | 342.70 | 1.0 | 13.535 | 13.520 | .111 |
| 86 | 14.161 | 62.8 | 2.1680E-07 | 342.70 | 1.0 | 13.669 | 13.655 | .104 |
| 87 | 13.560 | 62.8 | 2.1680E-07 | 342.70 | 1.0 | 14.068 | 14.081 | -.094 |
| 88 | 13.650 | 63.5 | 2.0259E-07 | 60.96 | 1.0 | 2.634 | 2.650 | -.609 |
| 89 | 13.169 | 59.3 | 3.3412E-07 | 60.96 | 1.0 | 2.716 | 2.725 | -.332 |
| 90 | 12.845 | 57.4 | 4.2147E-07 | 60.96 | 1.0 | 2.766 | 2.768 | -.080 |
| 91 | 12.009 | 53.7 | 6.5255E-07 | 60.96 | 1.0 | 2.904 | 2.865 | 1.329 |

TABLE VII.- COMPARISON OF BASIC DATA AND CURVE-FIT RESULTS

FOR SHOCK STANDOFF DISTANCE – Continued

(b) Nonspherical bodies

| Case | $V_\infty$, km/sec | Alt., km | $\rho_\infty$, g/cm$^3$ | $R_B$, cm | Axis ratio | $\delta_D$, cm | $\delta_C$, cm | Error, percent |
|---|---|---|---|---|---|---|---|---|
| 102 | 13.650 | 63.5 | 2.0259E-07 | 121.92 | 2.0 | 4.688 | 4.606 | 1.753 |
| 103 | 13.169 | 59.3 | 3.3412E-07 | 121.92 | 2.0 | 4.843 | 4.756 | 1.800 |
| 104 | 12.845 | 57.4 | 4.2147E-07 | 121.92 | 2.0 | 4.934 | 4.845 | 1.807 |
| 105 | 12.458 | 55.5 | 5.2997E-07 | 121.92 | 2.0 | 5.044 | 4.945 | 1.967 |
| 106 | 12.009 | 53.7 | 6.5255E-07 | 121.92 | 2.0 | 5.173 | 5.051 | 2.352 |
| 107 | 11.499 | 52.0 | 8.0413E-07 | 121.92 | 2.0 | 5.290 | 5.165 | 2.355 |
| 108 | 13.650 | 63.5 | 2.0259E-07 | 243.84 | 4.0 | 7.268 | 7.106 | 2.230 |
| 109 | 13.169 | 59.3 | 3.3412E-07 | 243.84 | 4.0 | 7.501 | 7.368 | 1.773 |
| 110 | 12.845 | 57.4 | 4.2147E-07 | 243.84 | 4.0 | 7.625 | 7.527 | 1.286 |
| 111 | 12.458 | 55.5 | 5.2997E-07 | 243.84 | 4.0 | 7.783 | 7.708 | .964 |
| 112 | 12.009 | 53.7 | 6.5255E-07 | 243.84 | 4.0 | 7.978 | 7.905 | .919 |
| 113 | 11.499 | 52.0 | 8.0413E-07 | 243.84 | 4.0 | 8.242 | 8.119 | 1.492 |
| 114 | 13.650 | 63.5 | 2.0259E-07 | 365.76 | 6.0 | 8.728 | 8.688 | .459 |
| 115 | 13.169 | 59.3 | 3.3412E-07 | 365.76 | 6.0 | 8.963 | 9.030 | -.751 |
| 116 | 12.845 | 57.4 | 4.2147E-07 | 365.76 | 6.0 | 9.178 | 9.240 | -.678 |
| 117 | 12.458 | 55.5 | 5.2997E-07 | 365.76 | 6.0 | 9.352 | 9.481 | -1.380 |
| 118 | 12.009 | 53.7 | 6.5255E-07 | 365.76 | 6.0 | 9.575 | 9.745 | -1.777 |
| 119 | 11.499 | 52.0 | 8.0413E-07 | 365.76 | 6.0 | 9.800 | 10.035 | -2.400 |
| 120 | 13.580 | 64.2 | 1.8447E-07 | 243.70 | 4.0 | 6.994 | 7.106 | -1.596 |
| 121 | 13.232 | 60.1 | 3.0232E-07 | 243.70 | 4.0 | 7.195 | 7.321 | -1.757 |
| 122 | 12.701 | 56.2 | 4.8433E-07 | 243.70 | 4.0 | 7.423 | 7.603 | -2.420 |
| 123 | 11.949 | 52.6 | 7.4351E-07 | 243.70 | 4.0 | 7.791 | 7.954 | -2.093 |
| 124 | 10.963 | 49.3 | 1.1199E-06 | 243.70 | 4.0 | 8.134 | 8.370 | -2.896 |
| 125 | 12.700 | 59.2 | 3.3958E-07 | 179.83 | 4.0 | 5.644 | 5.590 | .962 |

TABLE VII.- COMPARISON OF BASIC DATA AND CURVE-FIT RESULTS

FOR SHOCK STANDOFF DISTANCE – Concluded

(b) Nonspherical bodies – Concluded

| Case | $V_\infty$, km/sec | Alt., km | $\rho_\infty$, g/cm$^3$ | $R_B$, cm | Axis ratio | $\delta_D$, cm | $\delta_C$, cm | Error, percent |
|---|---|---|---|---|---|---|---|---|
| 126 | 12.254 | 55.4 | 5.3436E-07 | 179.83 | 4.0 | 5.817 | 5.767 | .853 |
| 127 | 11.611 | 51.9 | 8.1349E-07 | 179.83 | 4.0 | 6.063 | 5.985 | 1.286 |
| 128 | 13.161 | 61.0 | 2.6849E-07 | 231.64 | 4.0 | 7.094 | 6.967 | 1.788 |
| 129 | 12.767 | 57.1 | 4.3343E-07 | 231.64 | 4.0 | 7.370 | 7.190 | 2.441 |
| 130 | 12.190 | 53.4 | 6.7347E-07 | 231.64 | 4.0 | 7.545 | 7.469 | 1.003 |
| 131 | 11.398 | 50.0 | 1.0247E-06 | 231.64 | 4.0 | 7.947 | 7.812 | 1.701 |
| 132 | 13.467 | 64.2 | 1.8330E-07 | 262.12 | 4.0 | 7.840 | 7.661 | 2.285 |
| 133 | 12.909 | 59.2 | 3.3693E-07 | 262.12 | 4.0 | 8.073 | 7.998 | .933 |
| 134 | 12.220 | 55.5 | 5.2983E-07 | 262.12 | 4.0 | 8.408 | 8.356 | .616 |
| 135 | 11.295 | 52.0 | 7.9770E-07 | 262.12 | 4.0 | 8.847 | 8.785 | .699 |
| 136 | 13.050 | 61.1 | 2.6667E-07 | 252.98 | 4.0 | 7.724 | 7.624 | 1.290 |
| 137 | 12.592 | 57.2 | 4.2847E-07 | 252.98 | 4.0 | 8.220 | 7.891 | 3.997 |
| 138 | 11.932 | 53.6 | 6.6135E-07 | 252.98 | 4.0 | 8.336 | 8.225 | 1.329 |
| 139 | 11.052 | 50.3 | 9.9419E-07 | 252.98 | 4.0 | 8.695 | 8.623 | .832 |
| 140 | 12.700 | 59.2 | 3.3938E-07 | 249.94 | 4.0 | 7.788 | 7.706 | 1.048 |
| 141 | 12.254 | 55.4 | 5.3436E-07 | 249.94 | 4.0 | 8.013 | 7.966 | .585 |
| 142 | 11.611 | 51.9 | 8.1349E-07 | 249.94 | 4.0 | 8.396 | 8.289 | 1.279 |
| 143 | 13.016 | 62.0 | 2.3774E-07 | 231.64 | 4.0 | 7.075 | 6.985 | 1.275 |
| 144 | 12.723 | 58.1 | 3.8424E-07 | 231.64 | 4.0 | 7.276 | 7.176 | 1.368 |
| 145 | 12.281 | 54.4 | 6.0208E-07 | 231.64 | 4.0 | 7.484 | 7.414 | .930 |
| 146 | 11.656 | 50.9 | 9.2060E-07 | 231.64 | 4.0 | 7.845 | 7.708 | 1.742 |
| 147 | 10.819 | 47.6 | 1.3803E-06 | 231.64 | 4.0 | 8.238 | 8.057 | 2.196 |
| 148 | 12.909 | 59.2 | 3.3693E-07 | 179.83 | 4.0 | 5.594 | 5.543 | .908 |
| 149 | 12.220 | 55.5 | 5.2983E-07 | 179.83 | 4.0 | 5.820 | 5.773 | .808 |
| 150 | 11.931 | 56.6 | 4.6395E-07 | 219.46 | 4.0 | 7.114 | 7.065 | .685 |

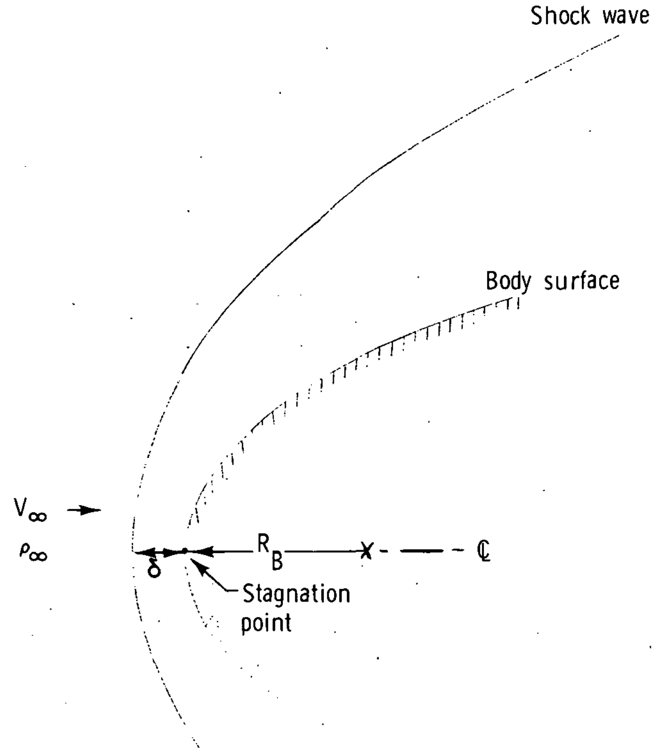


Figure 1.- Parameters of inviscid radiating flow-field solutions for stagnation region of a blunt body.

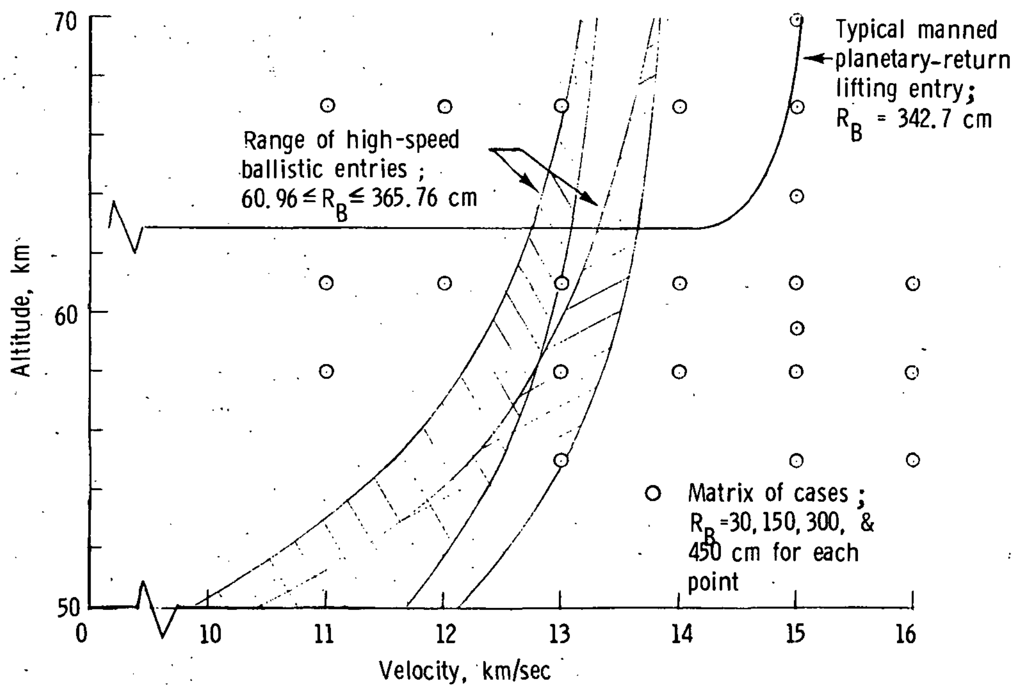


Figure 2.- Free-stream conditions and body sizes used in generating data to be curve fitted.

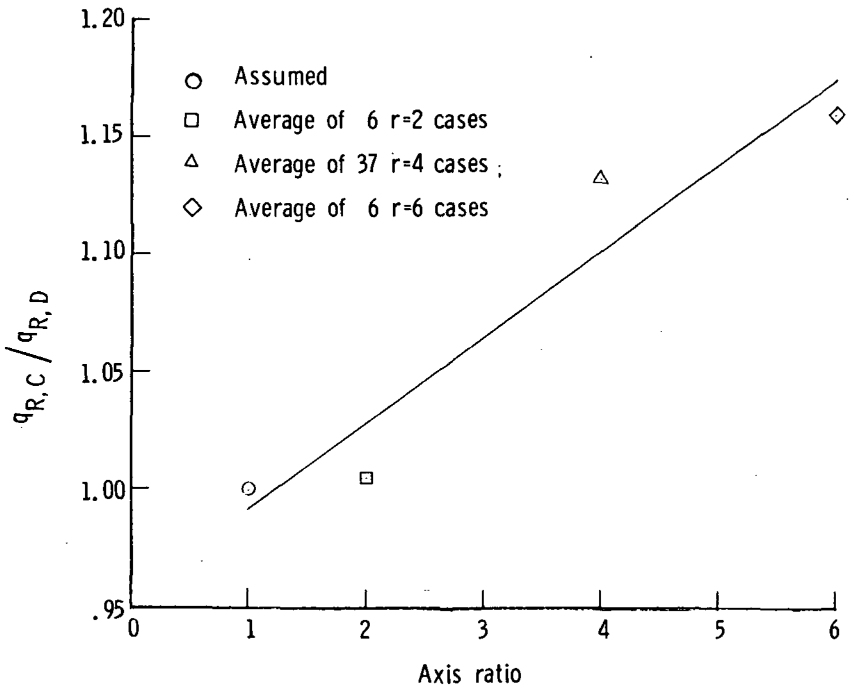


Figure 3.- Shape-factor correction for heating rate of elliptical bodies (free stream alined with semiminor axis).

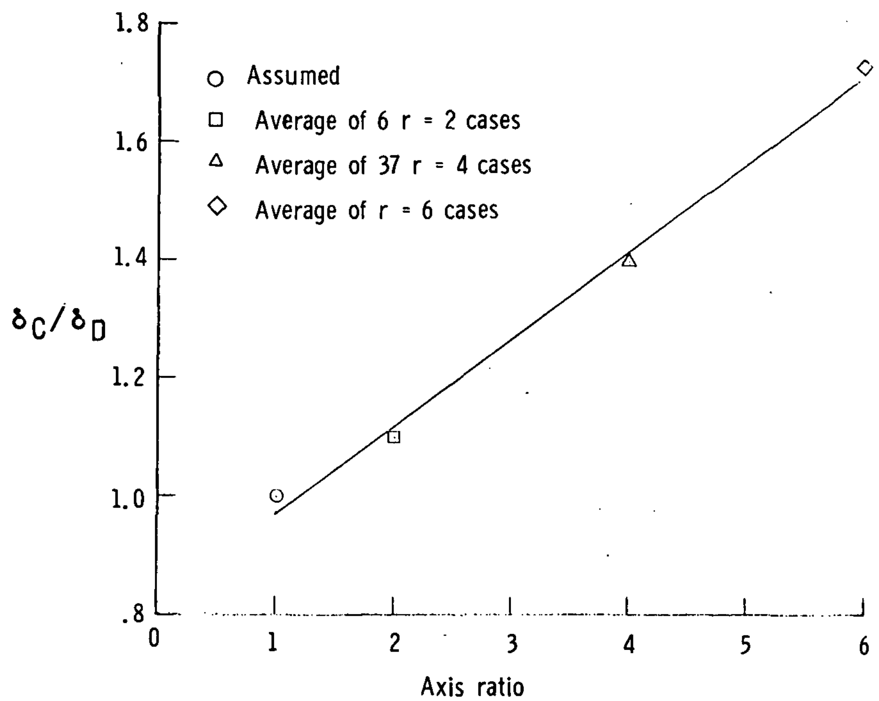


Figure 4.- Shape-factor correction for stagnation-point shock standoff distance of elliptical bodies (free stream alined with semiminor axis).

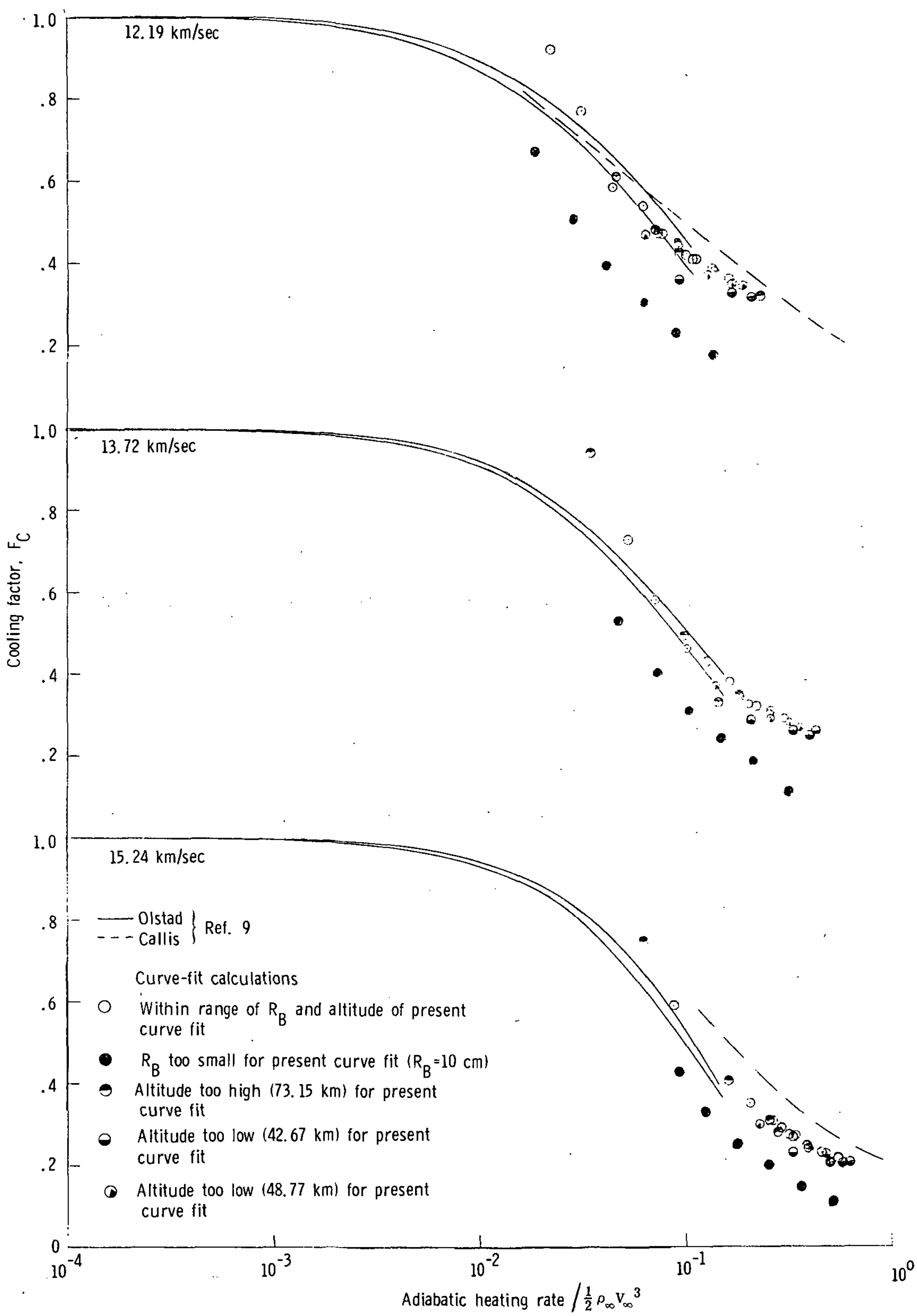


Figure 5.- Comparison of cooling-factor correlation curves from reference 9 with results of present curve fit for three velocities within the range of the present curve fit.

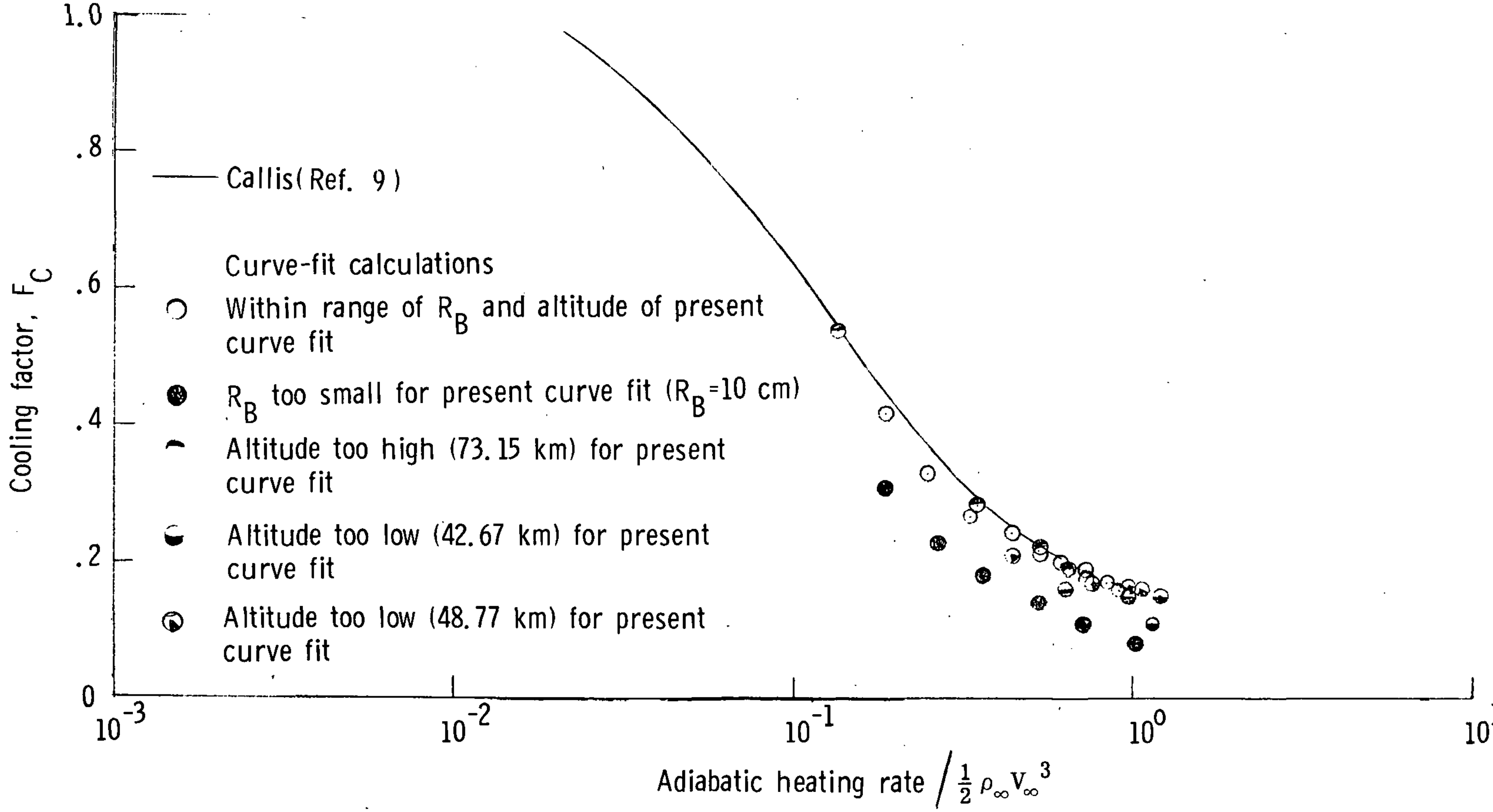


Figure 6.- Comparison of cooling-factor correlation curves from reference 9 with results of present curve fit for a velocity $(V_\infty = 18.28$ km/sec$)$ higher than those of the present curve fit.

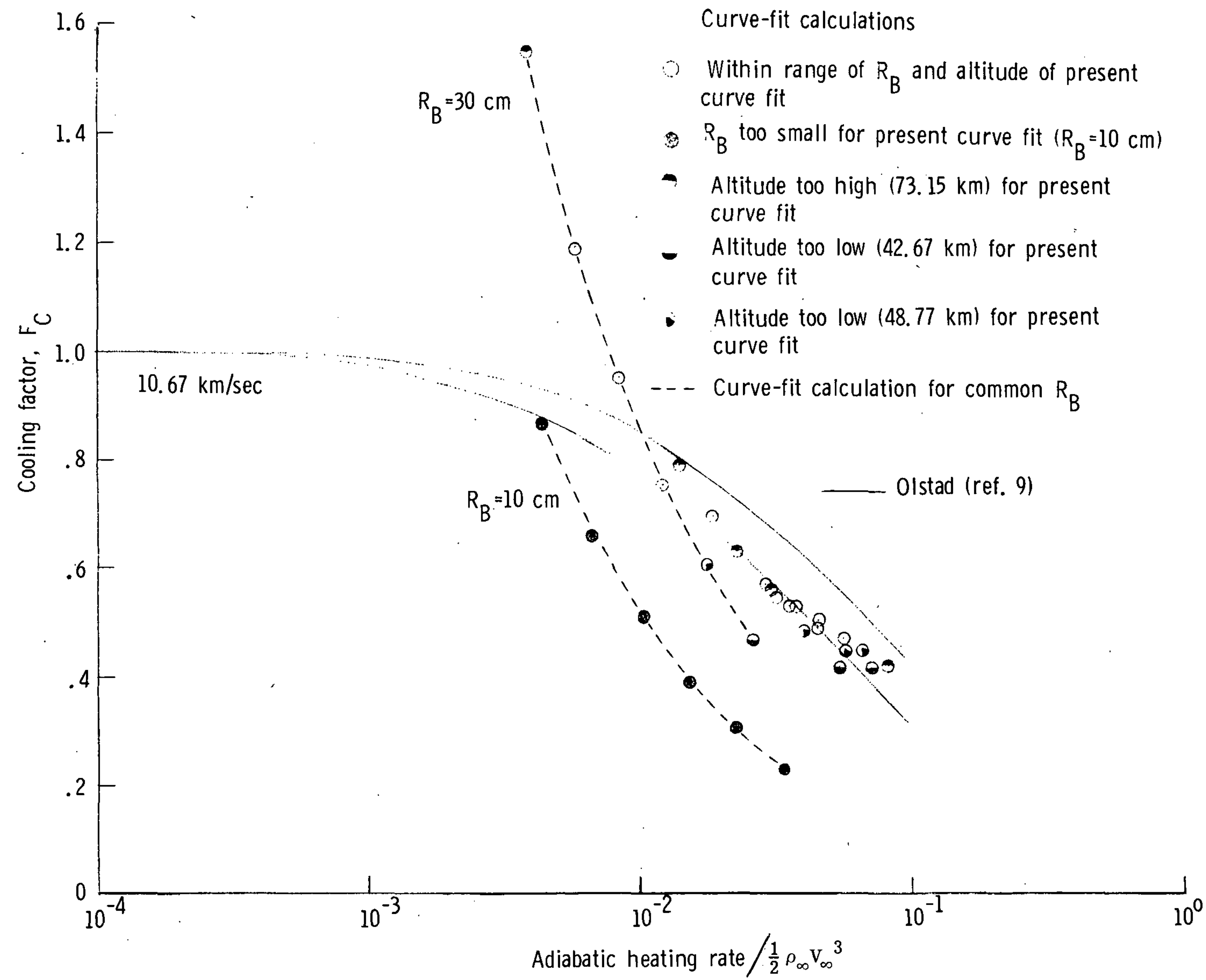


Figure 7.- Comparison of cooling-factor correlation curves from reference 9 with results of present curve fit for a velocity $(V_\infty = 10.67$ km/sec$)$ lower than those of the present curve fit.

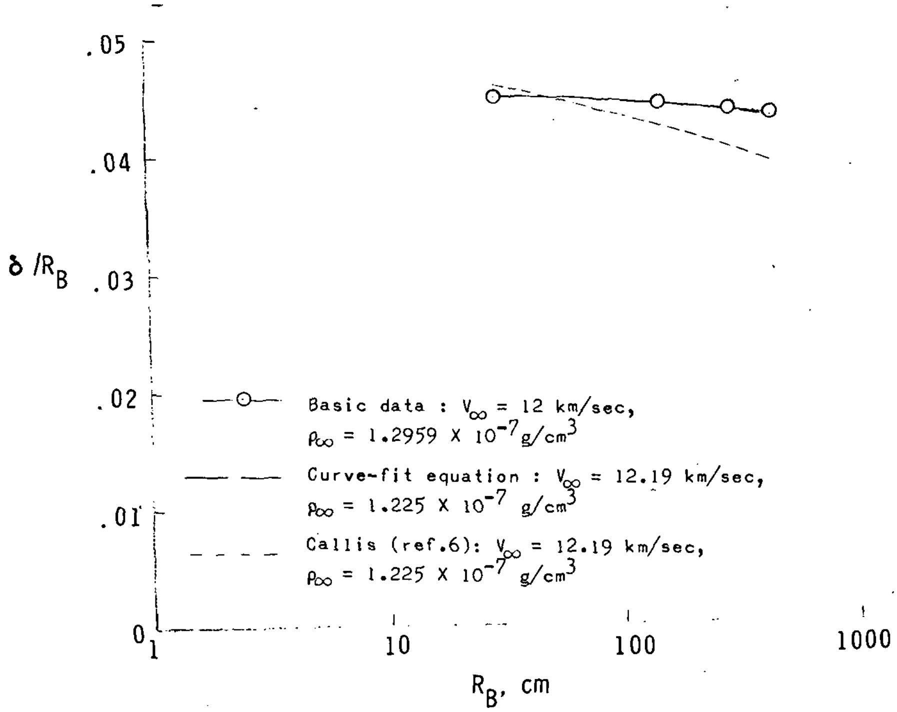


(a) Low velocity.

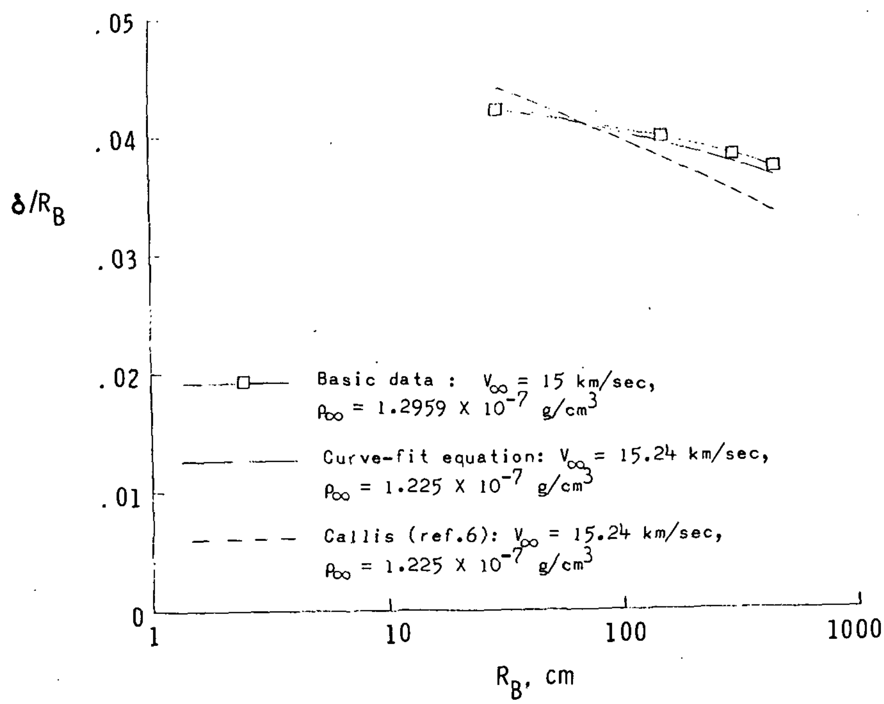


(b) High velocity.

Figure 8.- Comparison of shock standoff distances for basic data, curve-fit equation, and results of Callis (ref. 6).



NASA-Langley, 1974 L-9315

Page Intentionally Left Blank

NATIONAL AERONAUTICS AND SPACE ADMINISTRATION
WASHINGTON, D.C. 20546

OFFICIAL BUSINESS
PENALTY FOR PRIVATE USE $300

SPECIAL FOURTH-CLASS RATE
BOOK

POSTAGE AND FEES PAID
NATIONAL AERONAUTICS AND
SPACE ADMINISTRATION
451

U.S.MAIL

587 001 C1 U 33 740621 S00120ES
PHILCO FORD CORP
AERONUTRONIC DIV
AEROSPACE & COMMUNICATIONS OPERATIONS
ATTN: TECHNICAL INFO SERVICES
FORD & JAMBOREE ROADS
NEWPORT BEACH CA 92663

POSTMASTER: If Undeliverable (Section 158 Postal Manual) Do Not Return

*"The aeronautical and space activities of the United States shall be conducted so as to contribute . . . to the expansion of human knowledge of phenomena in the atmosphere and space. The Administration shall provide for the widest practicable and appropriate dissemination of information concerning its activities and the results thereof."*

—NATIONAL AERONAUTICS AND SPACE ACT OF 1958

# NASA SCIENTIFIC AND TECHNICAL PUBLICATIONS

TECHNICAL REPORTS: Scientific and technical information considered important, complete, and a lasting contribution to existing knowledge.

TECHNICAL NOTES: Information less broad in scope but nevertheless of importance as a contribution to existing knowledge.

TECHNICAL MEMORANDUMS: Information receiving limited distribution because of preliminary data, security classification, or other reasons. Also includes conference proceedings with either limited or unlimited distribution.

CONTRACTOR REPORTS: Scientific and technical information generated under a NASA contract or grant and considered an important contribution to existing knowledge.

TECHNICAL TRANSLATIONS: Information published in a foreign language considered to merit NASA distribution in English.

SPECIAL PUBLICATIONS: Information derived from or of value to NASA activities. Publications include final reports of major projects, monographs, data compilations, handbooks, sourcebooks, and special bibliographies.

TECHNOLOGY UTILIZATION PUBLICATIONS: Information on technology used by NASA that may be of particular interest in commercial and other non-aerospace applications. Publications include Tech Briefs, Technology Utilization Reports and Technology Surveys.

***Details on the availability of these publications may be obtained from:***

**SCIENTIFIC AND TECHNICAL INFORMATION OFFICE**

**NATIONAL AERONAUTICS AND SPACE ADMINISTRATION**

**Washington, D.C. 20546**